

Davis, Taylor and Davis, 2018**SUPPLEMENTARY MATERIALS****for**

Davis, W.J.; Taylor, P.J.; Davis, W.B. The Antarctic Centennial Oscillation: A Natural Paleoclimate Cycle in the Southern Hemisphere that Influences Global Temperature [*Climate*, 2017, doi: 10.3390/cli6010003]

1. Introduction

This Supplementary Materials (SM) document has two purposes. *First*, it details the methods used in this study. In this process potential artifacts from frequency aliasing and sample resolution are evaluated as minimal-to-absent and therefore are not the source of the documented changes in TOC_{350V} cycle frequency and amplitude. Similarly, noise introduced by vertical isotopic diffusion within ice cores and horizontal spatial variation in stable isotope concentration in snow, firn and ice are evaluated and considered negligible. Methods detailed include analysis of sources of error and uncertainty and mathematical methods for computing confidence limits for spectral periodograms.

Second, this SM presents SM Table 1, which contains all datapoints corresponding to the peak and trough of every TOC_{350V} cycle identified in the Vostok climate record from 226,408 to 0.149 Kyb1950 as reduced from original data contained in open-access databases based on the GT4 glaciological chronology [1, 2, 3]. SM Table 1 serves four purposes: 1) to enable independent confirmation of the data used in this study against the original data sources [1, 2, 3], 2) to permit independent confirmation of the most important results of this study, including TOC_{350V} cycle statistics (text-Table 1), 3) to document compliance of this analysis with the Nyquist-Shannon sample-frequency criterion, which ensures the absence of artifact from frequency aliasing, and 4) to support independent replication and further analysis of the results reported in this study.

2. Methods**2.1. Data Sources**

Open-source databases from Vostok (the GT4 glaciological chronology; [1, 2]) and three additional climate records dated using multiple stratigraphic markers (the Antarctic Ice Core Chronology of 2012, or the AICC2012 chronology; [4, 5]) provided the temperature-proxy data analyzed in this study. Values for CO₂ concentration were obtained from [1-3], although they are not used in the present study. Relatively highly-resolved CO₂ data from [3] were used also for the last ~2,500 years of the Holocene. Proxy data were downloaded from the paleoclimate databases available online from the World Data Center for Paleoclimatology, National Climate Data Center (NCDC), United States National Oceanic and Atmospheric Administration (NOAA) [6]. Computational data describing the 41 Ky obliquity/precession cycle of surface insolation at 65 °N were obtained from [7] (Supplementary Online Material).

Data evaluated include two isotopic water proxies of temperature anomaly expressed as deviations from the 1960-1990 global mean (ΔT), namely deuterium ($\delta^2\text{H}$, units of ‰) and oxygen ($\delta^{18}\text{O}$, units of ‰). Data summarized in SM Table 1 include atmospheric carbon dioxide (CO₂) measured from gas bubbles extracted from Vostok [1, 2] and EDC [3] ice cores (concentration, units of parts per million by volume or ppmv). Deuterium-based temperature-proxy data ($\delta^2\text{H}$) were

converted to estimated temperature anomaly and graphed as time series using the conversion factor $9‰ = 1^{\circ}\text{C}$ [1, 2, 8-11]. Reduction of temperature-proxy and CO_2 data to analytic format and color-coding of centennial-scale climate cycles according to the method of definition appear in SM Table 1.

2.2. Cycle Nomenclature

The climate-cycle nomenclature used here is based on classical-language prefixes and alphanumeric descriptors modified from Wunsch [12]. By this nomenclature each cycle of a characteristic repetition frequency is described beginning with the phrase "Temperature-proxy Oscillation" (TO) followed by three contiguous subscripts. The first subscript is the capitalized abbreviation of the term designating the order of magnitude of the cycle repetition period in years. The time periods, terms, and corresponding abbreviations used for the first subscript in this cycle nomenclature, respectively, are: less than one year, Intra-annual, I; yearly, Annual, A; tens of years, Deca, D; hundreds of years, Cento, C; thousands of years, Kilo, K; and millions of years, Mega, M. All contemporary climate cycles can be defined using the first five of these suffixes. The sixth suffix pertains to the multi-million-year climate cycles of the Phanerozoic Eon.

The second of the three suffixes to the acronym TO in this climate-cycle nomenclature is the numerical value of the average cycle period, if known, rounded to the nearest ten. The centennial-scale climate cycles documented in the present study occur at a mean period of 352 years over the 226.4 Ky time period in which they are identifiable (text-Table 1), which is rounded to 350. The period of the centennial-scale cycle detected in this study decreases over time, rendering the mean pertinent only to the entire 226.4 Ky time period over which it was measured. Mean period computed over shorter time segments differ from the overall mean by up to a factor of 3-4.

The third suffix to the acronym TO is either the capitalized letter "S" (Stationary time series) or "V" (Variable time series), which indicates whether or not the cycle is stationary or variable over time, if known. This suffix is required because some known climate cycles are paced by orbital forces, which for practical purposes are stationary time series, but most identified climate cycles are variable (non-stationary) time series, including the Antarctic Centennial Oscillation (ACO) documented in the present study as well as the Antarctic millennial AIM cycle that corresponds to the Bond cycle in the NH. The subscript "V" is appended to the cycle nomenclature as the third suffix if cycle period is variable and consequently the mean value depends upon the time segment chosen for calculating it.

Under this climate-cycle nomenclature, the ACO is termed the $\text{TO}_{\text{C}350\text{V}}$ cycle (Temperature-proxy Oscillation_{Centennial-scale 350 year mean period Variable}), while the millennial-scale cycle is termed the $\text{TO}_{\text{K}1500\text{V}}$ cycle. This nomenclature can be generalized to all climate cycles. Examples include the ~100,000-year MISs with quasi-regular period of 80-120 Ky ($\text{TO}_{\text{K}80-120\text{V}}$), decadal-scale cycles of unmeasured period (TO_{D}), etc. The terms "ACO" and $\text{TO}_{\text{C}350\text{V}}$ are used interchangeably throughout this paper and SM.

2.3. Frequency Aliasing

Constructing climate records entails first sampling the underlying continuous temperature (the original or "reference" signal) digitally using a sampling frequency sufficient to preserve the fidelity of the reconstructed proxy record in the desired bandwidth, in this case centennial. Oscillatory phenomena that are sampled at too low a frequency can contain aliasing artifact, in which a high-frequency component of the reference signal appears incorrectly as a lower-frequency alias. Quantitative methods for sampling and accurately reconstructing such periodic multiband

waveforms have been developed in information theory [13, 14, 15, 16] and extended to climate sciences by several investigators [e.g. 12, 17, 18, 19, 20, 21, 22, 23, 24, 25]. The minimum sampling frequency required to accurately digitize and reconstruct the underlying periodic reference signal is established by the Nyquist-Shannon sampling-frequency theorem [13, 14, 15]. According to this theorem, resolving the highest frequency contained in a multiband signal that is bandwidth-limited at the highest frequencies and sampled by equally-spaced datapoints requires a minimum of two sample datapoints per cycle (e.g., 16). Sampling frequencies less than two samples per cycle generate aliasing artifact, i.e., an artificial lower-frequency signal that is a reconstituted alias of higher frequencies [16]. For example, a centennial oscillation like the ACO requires sampling minimally at 50-year intervals to avoid aliasing artifact. Sampling at frequencies above the Nyquist-Shannon criterion, however, eliminates the artifact associated with frequency aliasing [e.g., 19, 20, 21], but does not necessarily preclude attenuation of the amplitude of the reconstructed signal as discussed below (see below, SM section 2. Methods, 2.7. Sources of Uncertainty, 2.7.2. Amplitude, p. 11).

Correct application of the Nyquist-Shannon sampling-frequency theorem has two mathematical prerequisites: equally-spaced sampling datapoints [13, 14] and [26] (equations 1-3 on p. 1565, where samples are "...spaced (1/2w) apart.") and an upper bandwidth limit that is known. The data analyzed in this study, and in most climate studies, generally meet neither of these two criteria. Although Vostok ice cores were sampled originally in lengths of one meter [1], samples are not equivalent in the time represented per sample owing to differential compression of the ice core with depth, i.e. sampling is "non-uniform" [15], which in theory limits or precludes aliasing artifact.

Over shorter time periods and at depths reflecting minimal or constant ice-core compression, however, samples may be more equally spaced in time. Over these shorter periods, therefore, compliance with the Nyquist-Shannon sampling-frequency criterion may be appropriate to minimize frequency aliasing. Similarly, it can be argued that the upper bandwidth of the reference signal is both limited and specified by firn and ice core dynamics that filter out cycles ranging from annual to 30 years in periodicity (see below, SM section 2.7.4. Stratigraphic Noise, p. 12). The present analysis therefore conservatively complies with the Nyquist-Shannon sampling-frequency criterion of at least two samples per cycle for all centennial-scale climate cycles evaluated in the present study. Meeting the Nyquist-Shannon frequency-sampling criterion was achieved by analyzing only that time period of the Vostok record over which the original sampling frequency exceeds the Nyquist-Shannon sampling-frequency criterion for every centennial-scale climate cycle identified, i.e., from 226.4 to 0.149 Kyb1950.

With the exception of older portions of the TD climate record, sampling resolution is higher for other (non-Vostok) AICC2012-synchronized climate records, precluding frequency aliasing artifact in the centennial bandwidth and requiring averaging (filtering) to yield sample resolutions that can be compared meaningfully with the Vostok temperature-proxy record. The sampling frequency of TO_{C350V} cycles from the Vostok GT4 chronology in this study is documented in SM Table 1 as the number of sample datapoints per warming and cooling phase of each TO_{C350V} cycle. The average number of sample points per ACO is six, three times the Nyquist-Shannon criterion.

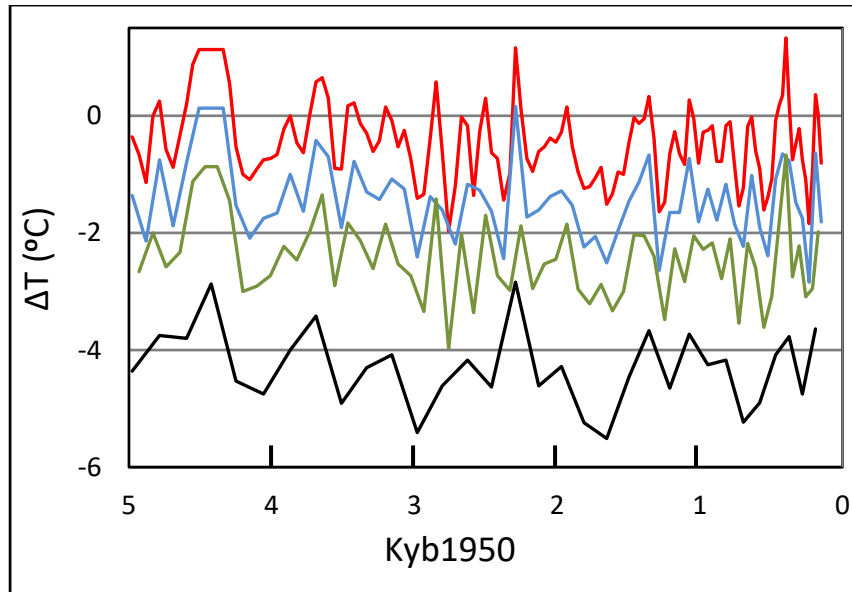
Aliasing variance contained in digitized climate records has been estimated empirically using the index of the ratio of averaging length (AL) to sample interval (SM) [20]. When the AL/SM ratio is less than 1, "considerable aliased variance can appear at all, even the lowest, frequencies." [20] (p. 3987). When the AL/SM ratio exceeds unity, however, little-to-no aliasing variance is observed. In the present study, the maximum averaging length of the Vostok climate record analyzed is 226.4 Ky while the measured sample frequency ranges from six to 24 samples per Ky, corresponding to sample intervals of 0.04 to 0.14 Ky. The AL/SM ratio for the entire Vostok climate record analyzed is therefore 1614-5648, three orders of magnitude above the range that is subject to significant frequency aliasing artifact. Shorter records with averaging lengths of five to seven Ky and SMs of a

few centuries are also analyzed in the present study. In these cases the AL/SM ratio is 15-20, still greater than unity by an order of magnitude and therefore also in a range that excludes significant frequency aliasing artifact. A conservative estimate of the percent of aliased variance in this study as assessed quantitatively using this empirical indicator was estimated from [20] (Figure 2, p. 3988) as < 0.5%.

Aliasing artifact was explored empirically by resampling the Vostok record at defined fractions of the original sampling frequency, accomplished by deleting every second sample point from the original sampling that comprises the Vostok GT4 temperature-proxy reconstruction. Using every other data point reduces the sampling frequency by half, which is expected under the Nyquist-Shannon theorem to generate lower alias frequencies if aliasing artifact is contained in the reconstructed waveform. Only the frequency of sampling, and not the time integrated into individual samples, is relevant to this resampling procedure. Over the last 5000 years, visible periodicity in the Vostok climate record occurs at nearly identical frequencies in records sampled at the original Vostok sampling frequency and resampled at half that frequency (SM Figure 1), demonstrating absence of frequency aliasing at both sampling frequencies.

Resampling at one-fourth the original frequency, accomplished by deleting three of every four sequential original sample datapoints, reduces sampling frequency well below the Nyquist-Shannon sampling-frequency criterion for centennial-scale reconstructions and simultaneously approximately doubles the returned period of the reconstructed waveform (SM Figure 1), as anticipated from frequency aliasing artifact and also from broadband filtering. Sampling below the Nyquist-Shannon sample-frequency criterion also yields moderate amplitude attenuation (SM Figure 1). The same resampling experiment was performed on the five-Ky time segments of the Vostok record from 20 to 0 Kyb1950 (not shown) and on older segments of the temperature-proxy record contained (not shown), with similar results. These findings demonstrate that frequency-aliasing artifact is minimal or absent at the original Vostok sampling frequency in respect to centennial-scale cycles, and on resampling at half the original frequency. These findings also illustrate potential frequency aliasing when sampling frequency declines below the Nyquist-Shannon sampling-frequency criterion, as expected.

Amplitude attenuation in the temperature-proxy record is possible and sometimes evident upon resampling the Vostok climate record at lower frequencies (e.g. SM Figure 1). This source of variance is discussed below in greater detail (SM section 2. Methods. 2.7. *Sources of Uncertainty, 2.7.2. Amplitude*, p. 11). The Vostok record of atmospheric CO₂ concentration was sampled originally at a lower sample frequency than the temperature proxy record and is inadequate to assure the detection of centennial-scale events without frequency aliasing under the Nyquist-Shannon sampling-frequency criterion. Centennial-scale periodicity in the paleoclimate gas record therefore cannot be addressed without more complex sub-Nyquist-Shannon analytic protocols, which were not implemented here.



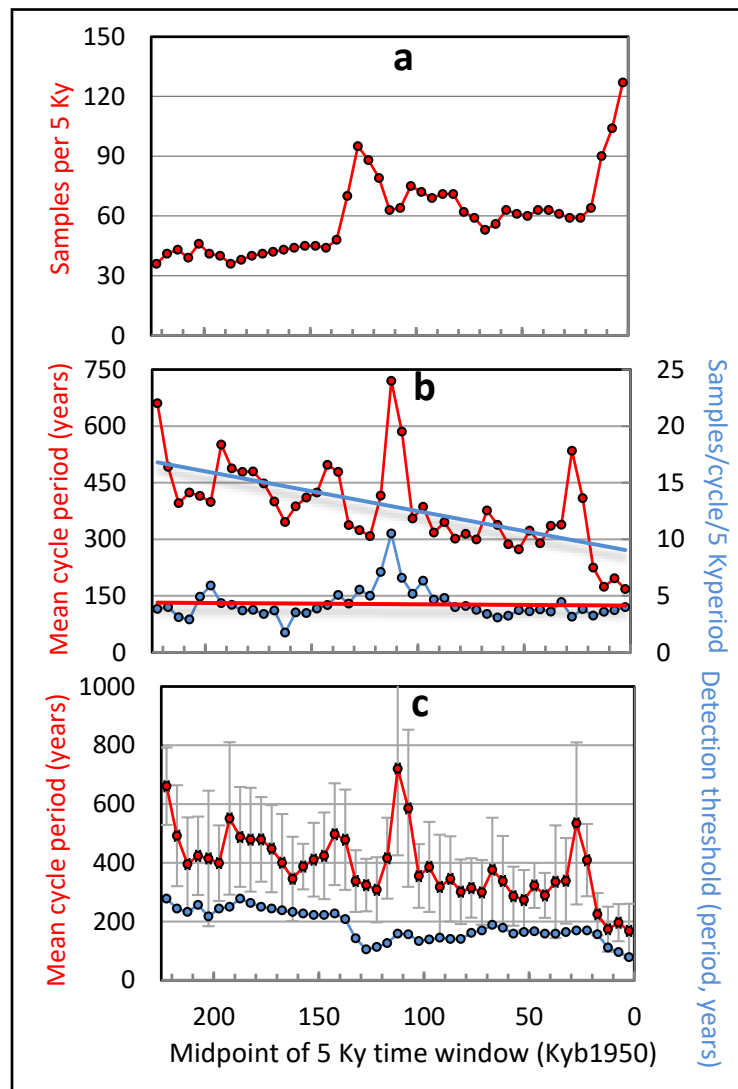
SM Figure 1. Periodicity of centennial-scale climate cycles in the Vostok climate record over the last 5 Ky displayed at different sampling frequencies. Red curve, all Vostok sample datapoints. Blue curve, even sample datapoints deleted. Green curve, odd sample datapoints deleted. Black curve, sampling frequency reduced to one-fourth the original, beneath the Nyquist-Shannon sampling-frequency criterion. The blue, green and black curves are shifted downward by 1 °C, 2 °C and 3 °C, respectively to render the curves visually distinct, requiring adjustment of the ordinate by comparable increments to create an accurate amplitude scale for the shifted curves.

2.4. Sample Resolution

To assess the impact of sample resolution in the GT4 Vostok chronology on the present results, mean sample frequency over five-Ky time windows was computed. This computation yields original sample frequencies of ~30 to 120 per five Ky or six to 24 per Ky (SM Figure 2a). The number of samples per TO_{C350V} cycle is relatively stable across the 226.4 Ky evaluated, at approximately five samples per cycle (SM Figure 2b, blue curve) with the exception of a peak at 110-120 Ky associated with a reduction in cycle frequency coincident with an obliquity/precession cycle peak (text-Figures. 9-12). Over the same time period the mean cycle period declines by a factor of two (SM Figure 2b, red curve). Cycle frequency therefore declines by 100% and fluctuates episodically by up to an order of magnitude (see main paper, section 3.Results) as sampling frequency remains relatively constant. TO_{C350V} cycle frequency is therefore independent of sampling frequency, i.e. the observed decline in cycle period is not attributable to a change in sample resolution.

The average cycle period detectable under the Nyquist-Shannon sampling-frequency criterion, computed by doubling the minimal qualifying sample frequency (2 per cycle) and converting to period, declines over the 226.4 Ky period evaluated here from ~300 to ~100 years (SM Figure 2c, blue curve). The mean TO_{C350V} cycle period over the same time period ranges from two to three times this threshold for detection of centennial-scale cycles in the absence of frequency aliasing artifact (SM Figure 2c, blue curve). The threshold for cycle detection under the Nyquist-Shannon sampling-frequency criterion lies outside the 96% confidence limits of cycle period (two standard deviations, or 2σ) (SM Figure 2c, red curve). The sample resolution available in the Vostok GT4 chronology is therefore greater than required to detect centennial-scale cycles over the 226.4-Ky period evaluated

in this study without inducing frequency-aliasing artifact or other resolution-related noise. The sample resolution is inadequate, however, to detect cycles on decadal time scales.



SM Figure 2. Sample resolution and corresponding Nyquist-Shannon centennial-scale cycle detection threshold over the Vostok climate record (GT4 chronology) (a) mean sample frequency per five Ky. (b) mean cycle period and samples per cycle. (c) mean cycle period compared with the minimum detectable cycle period consistent with the Nyquist-Shannon (N-Q) sampling-frequency criterion. Red and blue trendlines in (b) are fitted by the method of least squares.

The possibility that the observed increase in $\text{TO}_{\text{C}_{350\text{V}}}$ cycle frequency over the 226.4 Ky time period analyzed resulted from artifact associated with a sampling frequency too low to detect shorter cycles in older portions of the Vostok climate record (e.g., SM Figure 2a) is excluded by four related empirical results pertaining to sampling resolution and cycle period (SM Figure 2). First, cycle frequency and sample resolution are independent over long periods of the 226.4 Ky record analyzed here. For about half the record (from 130 to 20 Kyb1950), for example, the number of sample datapoints per unit time remains constant or increases slightly (SM Figure 2a) while $\text{TO}_{\text{C}_{350\text{V}}}$ cycle period over this same period declines by a factor of two, the same average rate of decline as

observed over the whole of the 226.4 Ky analyzed (SM Figure 2a, text-Figure 9a). Second, the number of sample datapoints per cycle remains relatively constant over the entire 226.4 Ky while TO_{C350V} cycle period decreases by at least a factor of two (SM Figure 2b), demonstrating independence between sample resolution and cycle period. Third, the Nyquist-Shannon sample-frequency criterion is exceeded for every TO_{C350V} cycle identified in this study (SM Figure 2c), on average by 300%. Fourth, rapid, short-term fluctuations in cycle period of several hundred percent occur while sample resolution remains unchanged (cf. text-Figure 9b with SM Figure 2a). We conclude that the observed variance in TO_{C350V} cycle period is not attributable either to frequency aliasing or to artifice stemming from too low or variable a sampling resolution.

2.5. Definition of Centennial-scale Cycles

Quantitative analysis of centennial-scale climate cycles in this study, and replication of our results, requires adherence to formal definitions of TO_{C350V} cycles. These definitions vary across the time period studied here depending on characteristics of the Vostok temperature-proxy record and the appropriateness of different definitions for describing specific TO_{C350V} cycle parameters. Cyclic events are parameterized fully by their amplitude and period, both of which are therefore encompassed in the following definitions of TO_{C350V} cycles. Three quantitative definitions of TO_{C350V} cycles were found essential to a full depiction of relevant TO_{C350V} cycle properties.

2.5.1. Definition 1

By the first definition, a TO_{C350V} climate cycle is any temperature-proxy oscillation, i.e., a warming followed immediately by a cooling, composed of a minimum of three sequential datapoints and exceeding 0.25 °C in amplitude. All TO_{C350V} cycles corresponding to definition 1 are labeled in bold black font in SM Table 1 and in all figures in which TO_{C350V} cycles are labeled. The temperature-proxy value of 0.25 °C was adopted as a lower limit on amplitude for definition 1 because it is easily discernible in the magnified temperature-proxy record, large enough to be considered a "significant" temperature anomaly, approximates the estimated 2 σ (96%) confidence limit for TO_{C350V} amplitude (0.29 °C, see below), and therefore can be interpreted unambiguously as a temperature signal rather than noise on the basis of amplitude alone. This first definition characterizes the majority (89.9%) of the 546 applicable TO_{C350V} cycles identified in this study (SM Table 1).

2.5.2. Definition 2

By the second definition, a TO_{C350V} climate cycle is any temperature-proxy oscillation, i.e., a warming followed immediately by cooling, that entails at least three sequential datapoints and lies between 0.045 °C and 0.25 °C in amplitude as determined from the converted temperature-proxy value. The lower limit of 0.045 °C is the smallest full TO_{C350V} cycle amplitude detected in the Vostok climate record from 226.4 to 0.149 Kyb1950. All cycles corresponding to definition 2 are labeled in bold red font accompanied by letters in SM Table 1 and in all pertinent figures. This second definition characterizes a minority (8.05%) of the applicable 546 applicable TO_{C350V} cycles. This less-restrictive definition could in principle include a small number of temperature-proxy excursions that correspond to statistical noise, but this possibility is considered unlikely because even the smallest such temperature excursions are accompanied by comparable and usually larger homologs in climate records from other drill sites evaluated (EDC, EDML, TD) (e.g., text-Figure 6). The differences in the amplitudes of homologous climate cycles could be caused by variable local

conditions at different Antarctic drill-sites [29] combined perhaps with small-amplitude variance caused by averaging (discussed below in this section).

2.5.3. Definition 3

By the third definition used in this study, a TO_{C350V} cycle is any positive inflection of the temperature-proxy record followed immediately by a negative inflection, with both phases superimposed on either a rising or falling background temperature-proxy curve. All TO_{C350V} cycles corresponding to definition 3 are labeled using bold blue font accompanied by letters (SM Table 1 and pertinent figures). This third definition encompasses 104 additional TO_{C350V} cycles beyond those encompassed in definitions 1 and 2, or 16.0% of the 650 identified TO_{C350V} cycles. This least-restrictive definition could also in principle include some climate events that constitute noise in the climate record, but this possibility is rendered less likely by the observed 1:1 matching of such small temperature excursions with larger homologous cycles at EDC, EDML and/or TD (e.g. text-Figures 6, 8). Definition 3 was used for the sole purpose of analyzing TO_{C350V} cycle period, where it was combined with definitions 1 and 2 for a combined sample size of 650 cycles. The sensitivity analysis described below shows that eliminating this definition and using definitions 1 and 2 only increased calculated mean period by ~15%.

2.5.4. Rationale for Multiple Cycle Definitions

Three definitions of TO_{C350V} cycles were used in this study because no single definition sufficed for all examples of TO_{C350V} cycles observed and their relevant properties. The combined use of all three definitions enables the most accurate estimate of TO_{C350V} repetition period because the combination is maximally inclusive of putative TO_{C350V} cycles. As noted, ignoring all cycles corresponding to definition 3 lowers the mean cycle frequency over the 226.4 Ky period evaluated by ~15%. Because definition 3 is limited to inflections in the temperature-proxy curve, however, it does not permit computation of "baseline" cycle amplitude as defined in this study (see below, next section). The third definition alone therefore also precludes computation of warming or cooling duration or rate for TO_{C350V} cycles, which can be determined only using the first and second definitions.

The primary distinction between the first two definitions is cycle amplitude. All of the relatively large-amplitude ACOs encompassed by definition 1 are presumably genuine climate signals, while some smaller cycles encompassed by definition 2 could contain or comprise noise. Use of all three definitions also enabled separate analysis of larger TO_{C350V} cycles (definition 1, ~90% of identified cycles) and smaller TO_{C350V} cycles (definition 2, ~10% of cycles). In a few TO_{C350V} cycles corresponding to definitions 1 and 2 (<1% of the total), peaks or troughs contained two or more successive datapoints of the same ΔT values. In these cases the time of the peak or trough was computed as the average of the time of occurrence of all datapoints corresponding to the same value of ΔT .

2.6. Definition of ACO Properties

Several properties of Vostok TO_{C350V} cycles were evaluated quantitatively in this study to achieve a broad array of descriptive statistics and corresponding quantitative constraints on mechanism(s) that are eventually proposed to underlie the ACO. These properties are described in this section together with the units and applicable cycle definitions.

- *repetition period*, the time from the onset of one TO_{C350V} cycle to the onset of the immediately successive TO_{C350V} cycle (trough-to-trough time) in units of years (definitions 1-3);
- *cycle amplitude*, one-half the temperature anomaly excursion of the warming phase plus one-half the temperature anomaly excursion of the cooling phase in units of °C (definitions 1 and 2). This "baseline" approach was adopted because TO_{C350V} cycles are often superimposed on ascending or descending background temperatures, which changes the starting temperature anomaly (baseline) for each phase of the corresponding TO_{C350V} cycle. Measuring baseline temperature following this procedure is not possible for cycles under definition 3 because both rising and falling phases of the cycle either increase (on a warming background) or decrease (on a cooling background), rendering cycle amplitude as defined here meaningless;
 - *cycle duration*, the time from the onset of a TO_{C350V} cycle to the onset of the next successive cycle in units of years (definitions 1 and 2 only). Cycle duration is in practice synonymous with the corresponding cycle period, since >99% of TO_{C350V} cycles are contiguous, i.e., one cycle terminates at the same datapoint at which the following cycle begins;
 - *warming duration*, the time from the onset (trough) of a TO_{C350V} cycle to the peak of the same cycle in units of years (definitions 1 and 2 only);
 - *cooling duration*, the time from the peak of a TO_{C350V} cycle to the end of the same cycle (i.e., the next trough) in units of years (definitions 1 and 2 only);
 - *warming rate*, the amplitude of the warming phase divided by its duration in units of °C/century (definitions 1 and 2 only);
 - *cooling rate*, the amplitude of the cooling phase divided by its duration in units of °C/century (definitions 1 and 2 only); and
 - *cycle symmetry*, which occurs when cooling and warming parameters are not discernibly different and therefore the ratio of cooling duration to warming duration, or the ratio of cooling rate to warming rate, approaches unity. Measures of cycle symmetry using ratios are unitless (definitions 1 and 2 only). Analysis of cycle symmetry is not included in this study but is relevant to future analyses of mechanisms underlying the ACO.

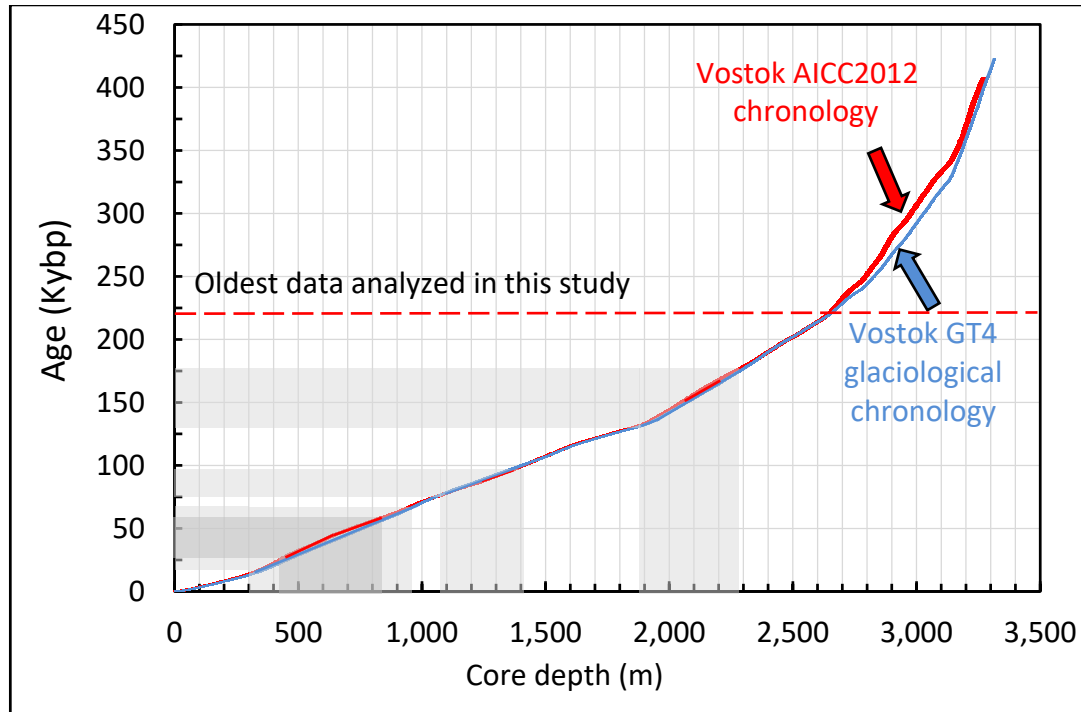
2.7. Sources of Uncertainty

Three classes of uncertainty or noise are considered in this section, associated with time, amplitude, and periodicity. Additional noise sources characteristic of ice-core data are also discussed, including measurement and stratigraphic error.

2.7.1. Time

The Vostok GT4 glaciological chronology [1,2] contains temporal uncertainties up to millennial scale over limited time ranges [e.g., 28-30]. These uncertainties were evaluated quantitatively by comparing the Vostok GT4 glaciological chronology with the most accurate Vostok paleoclimate age model available, AICC2012 [4, 5] (SM Figure 3). The most significant differences between the two age models are restricted to deeper (older) portions of the ice core beneath ~2,700 m (~250 Kybp) that lie outside the time frame analyzed in the present study. The more recent time period analyzed in the present study (226.4 to 0.149 Kyb1950) is characterized by less chronological difference between the two chronologies, ranging from small (<5%) to moderate (5-10%). The two periods evaluated in

the greatest detail in the present study, 70 to 63 Kyb1950 and 21 to 0.149 Kyb1950, show negligible difference (<5%) between the GT4 and AICC2012 Vostok chronologies (SM Figure 3).



SM Figure 3. Age model for the Vostok GT4 glaciological chronology (blue curve [1, 2]) plotted on the same scale as the age model of the AICC2012 Vostok chronology (red curve [4,5]). Light and dark shading in the plot area designate respectively negligible (<5%) and moderate (5-10%) differences between the GT4 and AICC2012 timescales. Unshaded regions comprise timespans characterized by little-to-no difference between the age models. The horizontal dashed red line denotes the oldest time period evaluated in this study, 226 Kyb1950. Analysis in the present study is limited to the period over which the two age models are nearly congruent (226,400 to 149 yb1950). Abbreviation: Kybp, thousands of years before present.

The largest difference between the chronologies (5-10%) within the time period covered by this study occurs from approximately five to 26 Kyb1950, a twenty-one Ky period that comprises 10.6% of the 226.4 Ky record analyzed in this study. The greater dating uncertainty of this time segment affects results limited to internal correlations of cycle properties and correlations with external variables including ΔT and CO_2 (not reported in the present paper). The emergence of discernible ($p < 0.05$) correlations for these variables over the entire 226.4 Ky record (not reported here) suggests that the greater chronological uncertainty over this small portion of the record did not influence significantly the conclusions reached in the present study.

All comparisons of $\text{TO}_{\text{C}_{350\text{V}}}$ cycles across different Antarctic drill sites were performed using climate records synchronized on the most accurate paleoclimate chronology available, AICC2012, including Vostok, EDC, TD and EDML. The chronology of these four climate records was established using multiple stratigraphic markers, which limits temporal uncertainty between these records to a reported ten to 500 years depending on the records compared and the time frame evaluated [4], as cited in the text of the main paper. Averaging of these records across time windows of different durations introduced minimum additional variance into the relative timing of $\text{TO}_{\text{C}_{350\text{V}}}$ cycles, measured empirically for all comparisons made as decadal in scale (see below, SM section 2. Methods, 2.8. Comparison of Climate Records from Different Sites, p. 13).

2.7.2. Amplitude

Digital sampling of a continuous periodic reference signal can attenuate the amplitude in reconstructed signals in inverse relation to sampling frequency (SM Figure 1). At the average sampling frequency of Vostok centennial-scale climate cycles over the 226.4 Ky evaluated, i.e., six datapoints or five equally-spaced intervals per cycle (SM Table 1), the separation between sampling points on a centennial-scale sinusoidal signal expressed in degrees of phase angle difference is 72° . Maximum cycle attenuation occurs when sampling intervals are equidistant from a peak or trough, or distributed symmetrically at either 324° and 36° (peaks) or 144° and 216° (troughs). Only one of these conditions need be considered because symmetrical distribution of two sample points across a peak at 0° of phase implies a sample point at 180° while distribution across a trough implies a sample point at 0° . In either case the corresponding maximum amplitude attenuation is $\sim 20\%$ of the maximum reference signal amplitude.

Since the underlying reference signal contains variance and sampling intervals are typically non-uniform, the maximum amplitude attenuation assuming random positioning of sample points on the underlying reference cycle is probably less than 20%, comprising a moderate source of variance in the reconstructed amplitude of Vostok TO_{C350V} cycles. Cycles with fewer sample datapoints may show greater amplitude attenuation, while cycles with more datapoints are expected to show less. Since the Vostok sampling frequency is relatively constant over time periods analyzed (SM Figure 2b, blue curve), amplitude attenuation is presumably unrelated to sample age and therefore cannot be responsible for the observed change in amplitude of ACO cycles over time. Empirical evidence for minimal attenuation of TO_{C350V} amplitude is presented in the main paper, section 3. Results, 3.6. *ACO Amplitude*, p. 19.

Variance in δ^2H temperature-proxy records from the Antarctic, expressed as one 1σ , has been measured and computed as 0.5‰ at EPICA Dome C on the EDC3 chronology [31] and 1.3‰ at Vostok on the GT4 chronology [11]. The corresponding 2σ confidence limits assuming a normal distribution are $1.0\text{--}2.6\text{‰}$. Several investigators [1, 4, 9, 10, 11] have measured the slope of the ratio of δ^2H to temperature as $9\text{‰}/^\circ\text{C}$, the basis of the temperature conversions applied to the transformation of Vostok δ^2H temperature-proxy data to ΔT used here [e.g., 1, 2]. The 2σ confidence limits for TO_{C350V} cycle amplitude converted to temperature anomaly is therefore $0.11\text{--}0.29\text{ }^\circ\text{C}$. Larger TO_{C350V} cycles, i.e. $0.29\text{ }^\circ\text{C}$ and greater, are therefore distinguishable from noise on the basis of amplitude alone. Smaller TO_{C350V} cycles that lie outside the estimated 2σ confidence limit cannot be distinguished from noise on the basis of amplitude alone. The distribution of TO_{C350V} cycle amplitude is such that $\sim 6\%$ of Vostok TO_{C350V} cycles lie outside the 2σ confidence limit for TO_{C350V} cycle amplitude of $0.11\text{ }^\circ\text{C}$, i.e., $\sim 94\%$ of TO_{C350V} cycles lie within this limit.

Most (99.01%) identified TO_{C350V} cycles are less than one Ky in duration and most (99.63%) are less than $3\text{ }^\circ\text{C}$ in amplitude. The majority (79.12%) of TO_{C350V} cycles are less than $1\text{ }^\circ\text{C}$ in amplitude, although the steady increase in TO_{C350V} cycle amplitude during the 226.4-Ky time period analyzed in this study implies that such small amplitude cycles occur mainly in older portions of the Vostok record. Separate analyses were performed using all TO_{C350V} cycles corresponding to definition 1 alone, definitions 1 and 2 combined, and all three definitions combined (period only), with conclusions similar to those reported here with the exception of repetition period, which as noted was approximately 15% larger when definition 3 was excluded. This sensitivity analysis showed that incorporating the smallest-amplitude TO_{C350V} cycles into the analysis based on the least-restrictive definitions of TO_{C350V} cycle amplitude did not alter the conclusions of this study materially, i.e., the results reported here are relatively insensitive to the definition of cycle amplitude.

2.7.3. Periodicity

A primary potential source of uncertainty in sampling periodic signals is aliasing artifact, which as detailed above is negligible or absent in this study (SM section 2. Methods. 2.3. *Frequency Aliasing*, p. 2 and SM Figures 1 and 2). The remaining potential uncertainty related to periodicity, and implicitly to the existence of TO_{C350V} cycles, is the possibility of irregular "bursty" fluctuation of the temperature-proxy record, i.e. variation of temperature-proxy in which the period of temperature-proxy cycles is distributed randomly over time. Among the usual tests for nonrandom periodicity in a potentially-periodic system are spectral density analysis and auto- and cross-correlation, although as noted in the main paper, this approach is not technically applicable to a non-stationary time series.

Spectral density analysis has been applied in previous studies of the Holocene in most Antarctic temperature-proxy records [e.g., 32] (their Figure 6, p. 356). That previous analysis disclosed small but discernible peaks at frequencies corresponding to TO_{C350V} cycles as defined here (100 to 400 years in period). These spectral density peaks are evident in all of the Antarctic climate records evaluated in this earlier study, suggesting that these cycles are distributed broadly across Antarctica. The present results confirm and extend those previous conclusions (text-Figures 2, 3, 4 and 7).

Lagged (serial, progressive) auto- and cross-correlation was done for select, representative time frames of the climate records studied here. In most cases time frames were first high-pass filtered and every datapoint comprising each TO_{C350V} cycle was normalized to a baseline of zero. Larger amplitude signals and longer repetition periods were thereby removed from the Vostok temperature-proxy record by extracting TO_{C350V} cycles defined as above from the remainder of the temperature-proxy record and evaluating them as a separate time series. To exclude longer periods, corresponding portions of the time series containing TO_{C350V} cycles to be evaluated for periodicity were normalized cycle-by-cycle and point-by-point to a common baseline by setting the first datapoint of each identified TO_{C350V} cycle equal to $\Delta T = 0$ °C through subtraction from its ΔT value of the measured difference from zero. The same arithmetic operation was performed iteratively on every successive datapoint of the corresponding TO_{C350V} cycle, initializing each cycle to a baseline of zero while preserving its waveform and simultaneously filtering out longer cycles. Sequences of filtered and temperature-normalized TO_{C350V} cycles were then subjected to progressive lagged autocorrelation analysis. This process of systematic removal of lower-frequency signals prior to autocorrelation is mathematically indistinguishable from high-pass filtering in the centennial bandwidth.

2.7.4. Stratigraphic Noise

The temperature-proxy record stored in frozen stable isotopes is subject to non-climate variance [33, 34, 35]. There are two general classes of such systematic error; pre-depositional and post-depositional. The former is atmospheric and human in origin while the later is associated physical processes that take place after snow has been incorporated in firn or in shallow cores. The two most important post-depositional classes of error associated with ice-core data are noise in measurement and stratigraphic noise. Measurement error is considered minor, estimated at ~1% [34] and therefore not considered here. Stratigraphic error is an order of magnitude greater [34].

The two most significant sources of stratigraphic error are vertical isotope diffusion and local horizontal isotope variation. Vertical isotope diffusion occurs in surface snow by vapor exchange with the atmosphere [36] and in firn by movement of water vapor prior to firn pore closure [33], and in shallow ice by migration through single ice crystals and their junctions [33]. Firn depth (age)

varies over the Antarctic as a function of local conditions and particularly with variation in snow accumulation from about 40–60 m (<50 years old) in high-accumulation coastal areas such as EDML to >100 m (2,000 years old at pore closure) in low-accumulation sites such as Vostok and EDC [37]. As firn densifies with depth and becomes progressively more compressed as ice, the uppermost layers can continue to be affected by moderate differentials in isotope diffusion with depth, in which stable isotopes used as temperature proxies migrate vertically as much as a few cm [33]. Modeled diffusion lengths decrease with depth, stabilizing at about 6 cm at Dome C at a depth of about 150 m [33] (their Figure 2, p. 129), which is about 50 m above the ice surface. Such diffusion smoothes high-frequency cycles reflected in temperature-proxy records in proportion to diffusion length [33].

As a consequence, annual cycles measured with increasing depth decline by two orders of magnitude in amplitude by a depth of about 70 m in shallow-core temperature-proxy data at the North Greenland Ice Core Project (NGRIP) [33] (Figure 3, p. 130). Firn diffusivity is an order of magnitude smaller for $\delta^2\text{H}$ than $\delta^{18}\text{O}$, however, owing to a lower vapor ice fractionation constant [33]. Since $\delta^2\text{H}$ is used as a temperature proxy at Vostok, the smoothing of high-frequency signals with increasing firn depth is less. Modeling isotopic diffusion suggests that these processes do not affect long-term low-frequency (multi-decadal and above) climate information contained in the temperature record of deep ice cores, but nearer the surface annual cycles used for dating can weaken and vanish with depth measured in meters to tens of meters, particularly for $\delta^{18}\text{O}$ at low accumulation sites.

Decadal and centennial cycles are affected less by isotope diffusion than annual and interannual cycles. Because the present study evaluates centennial signals and uses $\delta^2\text{H}$ as a temperature proxy at the low-accumulation Vostok site, isotope diffusion is unlikely to represent a significant source of noise, particularly at depths beneath the firn. On the other hand the possibility of some isotope diffusion noise in the temperature-proxy records of the recent Holocene, limited probably to the last 2,000 years, cannot be excluded. Since the present study covers 226.4 Ky, isotopic diffusion cannot explain the long-term, large-scale changes in the amplitude and frequency of centennial-scale temperature-proxy fluctuations reported here. Because the same trends are visible also during the Holocene (text-Figure 1), it seems unlikely that noise from isotope diffusion affects significantly any conclusion of this study.

The second major potential stratigraphic source of error in ice-core stable isotope data is local and regional horizontal variation in isotope concentration caused by snow drifting, erosion at the surface and irregular deposition [34, 35, 38, 39]. Concentrations of stable isotopes in one-m trenches and snow pits [39] separated horizontally by several tens of meters, and firn cores separated by kilometers [35] show substantially different stable isotope concentrations, and these differences can in principle be reflected vertically as firn densifies. Lack of correlation in stable isotope concentrations between adjacent snowpits characterizes decadal time scales, but significant correlations between adjacent cores begin to emerge on timescales larger than 30 years [40]. A common feature of all the studies cited here is that differences in local concentrations of stable isotopes disappear when integrated over a period of a few decades. Therefore, such local differences are unlikely to introduce significant variance into the interpretation of centennial-scale oscillations in stable isotopes frozen in deep ice cores.

2.8. Comparison of Climate Records from Different Sites

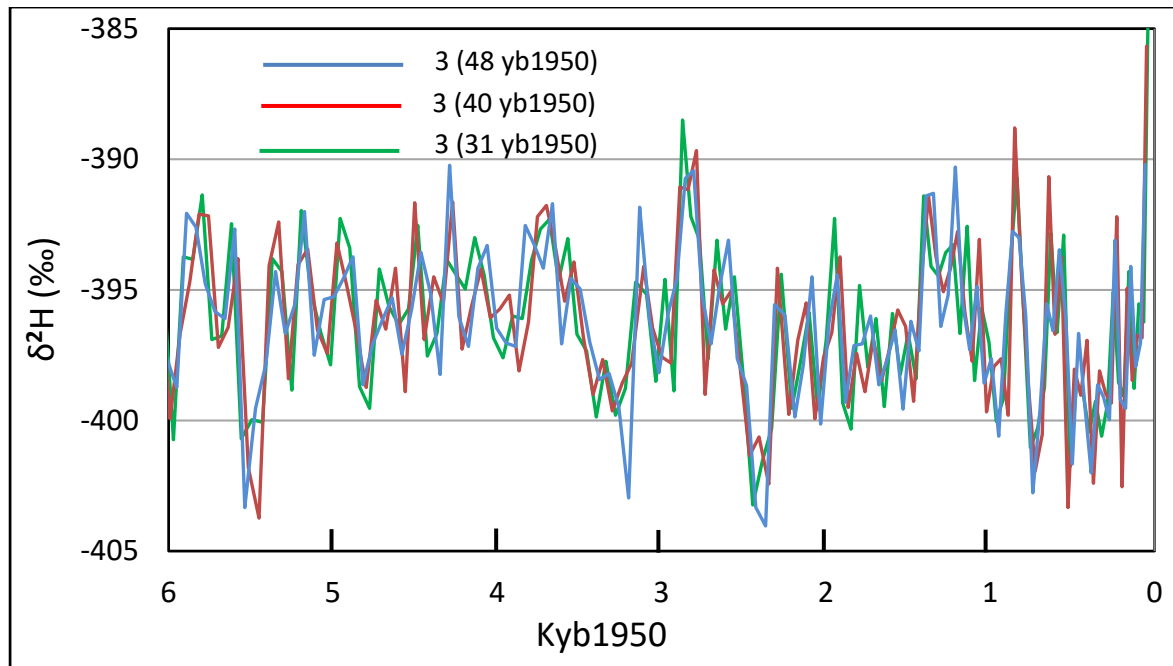
To determine whether $\text{TO}_{\text{C}_{350\text{V}}}$ cycles occur at Antarctic sites other than Vostok, climate records from the four Antarctic drill sites synchronized on the AICC2012 chronology were compared across defined time periods. This approach of waveform matching has been used by previous investigators to associate AIMs in the SH with corresponding D-O events in the NH [4, 41, 42]. In the present

study this method was restricted to comparison of signpost TO_{C350V} cycles, i.e., ACOs that are the most readily and objectively recognizable by their close association with other well-established climate events such as AIMs, the Last Glacial Maximum (LGM), the Antarctic Cold Reversal (ACR) etc. Remaining (non-signpost) TO_{C350V} cycles were matched across records based on objective variables: position in the sequence, number of cycles, waveform, and relative amplitude. Non-signpost TO_{C350V} cycles were generally not utilized for quantitative matching across records because their identification typically required more subjective decisions. They are nonetheless connected by gray connector lines in some text figures to illustrate the coherency (1:1 matching) of all Antarctic centennial cycles, which exceeds 98% of all cycles identified, signpost and non-signpost.

Accurate comparison of records reconstructed from different sampling frequencies used in the four AICC2012-synchronized Antarctic climate records required normalization of records to approximately equivalent sample resolutions to produce comparable frequency filtering. Of the four climate records compared, Vostok was sampled originally at the lowest sampling frequency, requiring averaging of the other three AICC2012 records, EDC, EDML, and TD to permit meaningful comparisons with Vostok. To enable accurate comparison of comparably-filtered climate records with Vostok, a simple arithmetic protocol was found to be effective. By this protocol, the number of samples per unit time was measured for each non-Vostok record to be compared with Vostok and the ratio of sampling frequency of the Vostok versus non-Vostok record was computed over the corresponding time periods. This ratio was used as the optimal bin width for averaging non-Vostok records to achieve the most accurate possible comparison of Vostok with non-Vostok climate records.

To illustrate this protocol, the EDC record over the period from six to 0.149 Kyb1950 contains 424 original sample datapoints, while the Vostok record over the same time period contains 183 original sample datapoints. The sample resolution ratio as defined above is therefore 424/183, or 2.3. Accordingly, in order to apply comparable averaging (filtering) to the EDC record for accurate comparison with the Vostok record over the same time period, the EDC record was first averaged in bin widths of both 2 and 3 to bracket the computed resolution ratio of 2.3 (SM Figure 4). Both bin widths produced high coherency between Vostok and EDC, i.e. optimal one-to-one matching of TO_{C350V} cycles, and hence both bin widths were used here to compute EDC averages. The same method was applied to ensure accurate and comparable comparison of all other climate records with Vostok.

Once the optimal averaging bin width was determined as above for each comparison between different climate records, the averaging process was refined further by evaluating the full range of possible start dates for application of the averaging protocol. The maximum number of unique start-dates for computing each average record is equal to the number of samples comprising the optimal computed bin width, e.g. two or three for the EDC record for the time period from six to 0 Kyb1950. As expected, averaging at different start dates results in identical periodicities within a reconstructed (averaged) record, but is characterized by decadal variance in latency between TO_{C350V} peaks (SM Figure 4). Averaging using different start dates therefore introduces a slight "jitter" or variance into computed differences in peak times. This variance, although small (<10%), is taken into account here when evaluating the relative timing of peaks (the latency between TO_{C350V} peaks at Vostok to homologous peaks in non-Vostok records) across different AICC2012 climate records. As a consequence of using these methods, replication of the results of different comparisons between climate records reported here requires using the same averaging protocol, i.e., the same averaging bin widths and the same start dates, which are accordingly reported in all relevant figure legends.



SM Figure 4. Variance from different averaging algorithms applied to the temperature-proxy record of EPICA Dome C over the time period from six to 0 Kyb1950. The key shows the averaging bin width (in all cases three) followed in parentheses by the start date for the averaging. Comparison of climate records using different averaging algorithms introduces decadal variance in the relative timing of cycle peaks. Replication of results comparing different climate records in the main text therefore requires using the same averaging protocol (bin width and start date), which is consequently reported in all pertinent figure legends in the main paper. Abbreviations: $\delta^2\text{H}$, deuterium excess (temperature proxy); yb1950, years before 1950.

2.9. Orbital Cycles

Summertime insolation energy at 65°N is generated almost exclusively by the obliquity cycle at insolation thresholds for glacial ablation less than 250 W/m^2 and varies equally with the obliquity and precession cycles at a threshold of 340 W/m^2 [7, 43]. The glacial ablation threshold value used here, $\tau = 325\text{ W/m}^2$, therefore, corresponds to insolation energy flux derived nearly equally from obliquity and precession with a weak bias toward obliquity. The results of this study are in any case relatively insensitive to the glacial ablation threshold chosen since the computed summertime insolation at 65°N is relatively independent of this threshold [7, 43]. The use of insolation computed for 65°N follows the same convention used previously [1] and does not affect the results reported here, which depend only on the observation that insolation from orbital cycles is cyclic and global in extent.

2.10. Spectral Analysis

The SAS JMP software used for spectral power analysis uses Fisher’s Kappa Test Statistic as a white-noise test. This statistic, κ , returns the probability that the distribution analyzed is generated by Gaussian (random) white noise against the alternative hypothesis that the spectral distribution is nonrandom. Kappa is the ratio of the maximum value of the periodogram, $I(f(x))$, to its average value. The probability (Pr) of observing a larger κ if the null hypothesis is true is given by:

$$\Pr(k > \kappa) = 1 - \sum_{j=0}^q (-1)^j \binom{q}{j} \left[\max\left(1 - \frac{jk}{q}, 0\right) \right]^{q-1} \tag{1}$$

where $q = N / 2$ if N is even and $q = (N - 1) / 2$ if N is odd. This probability is reported along with the corresponding κ value in the figure legends of the main paper for all spectral analyses done.

To compute confidence limits for periodograms, we used the Fourier series approximation of a $2L$ -periodic functions $f(x)$. Fourier’s Theorem states that all periodic functions can be approximated as weighted sums of sines and cosines of the harmonic frequencies of $f(x)$. All $2L$ -periodic functions $f(x)$ that are piecewise differentiable on an interval $[-L, L]$ exhibit a Fourier series approximation described by equation (2).

$$f(x) \approx a_0 + \sum_{n=1}^N a_n \cos\left(\frac{n\pi x}{L}\right) + \sum_{n=1}^N b_n \sin\left(\frac{n\pi x}{L}\right) \tag{2}$$

where

$$a_0 = \frac{1}{2L} \int_{-L}^{-L} f(x) dx \tag{3}$$

$$a_n = \frac{1}{L} \int_{-L}^{-L} f(x) \cos\left(\frac{n\pi x}{L}\right) dx \tag{4}$$

and

$$b_n = \frac{1}{L} \int_{-L}^{-L} f(x) \sin\left(\frac{n\pi x}{L}\right) dx \tag{5}$$

The weights a_n and b_n are the *Fourier coefficients*. The average of $f(x)$ is a_0 , and $b_0 = 0$ because $\sin(0) = 0$. The Fourier coefficients are themselves weighted averages of $f(x)$, where the weights are again sines and cosines of the harmonic frequencies.

Under additional well-established conditions, the Fourier series converges to $f(x)$. That is,

$$a_0 + \sum_{n=1}^N a_n \cos\left(\frac{n\pi x}{L}\right) + \sum_{n=1}^N b_n \sin\left(\frac{n\pi x}{L}\right) \xrightarrow{N \rightarrow \infty} f(x) \tag{6}$$

and $f(x)$ can be approximated to arbitrary precision by increasing N . The harmonics H of $f(x)$ are the innermost arguments in the Fourier theorem, namely the set

$$H = \left\{ \frac{n\pi x}{L} \mid n = 1, 2, \dots, N \right\} \tag{7}$$

Because $f(x)$ has period $2L$, it has frequency defined by equation (8)

$$\lambda = 1/2L, \text{ and } \frac{n\pi x}{L} = \frac{n2\pi x}{2L} = n2\pi\lambda x \tag{8}$$

If the angular frequency $\omega = 2\pi\lambda$, then

$$H = \{n\omega x \mid n = 1, 2, \dots, N\} \tag{9}$$

The set of harmonics are the integer multiples of the primary frequency of $f(x)$. To see that only periodic functions with harmonic frequencies are admissible as summands in the Fourier series, note that all other periodic functions will corrupt the frequency of the composite when summed. To preclude frequency corruption, the period of both summands must restart exactly when the longer period restarts. This can only occur with integer multiples of the primary frequency. Otherwise the summand must have a longer period, as synchronous restart then occurs at the least common multiple of both the frequencies (which may not even exist, in which case the sum is aperiodic).

Furthermore, the sines and cosines of the harmonic frequencies are mutually orthogonal, and therefore uncorrelated. That is, all their dot products are all zero.

$$\int_{-L}^L \cos\left(\frac{n\pi x}{L}\right) \cos\left(\frac{m\pi x}{L}\right) dx = 0, \int_{-L}^L \sin\left(\frac{n\pi x}{L}\right) \sin\left(\frac{m\pi x}{L}\right) dx = 0 \text{ when } \forall n \neq m \tag{10}$$

and

$$\int_{-L}^L \cos\left(\frac{n\pi x}{L}\right) \sin\left(\frac{m\pi x}{L}\right) dx = 0 \text{ when } \forall n, m = 1, 2, \dots \tag{11}$$

where n and m are positive integers.

This uncorrelated property is required for regressors, and suggests estimating the Fourier coefficients by minimizing the sum of squared errors. Adapting the Fourier series approximation to a discrete time series,

$$y(t) = a_0 + \sum_{n=1}^N a_n \cos\left(\frac{n\pi t}{L}\right) + \sum_{n=1}^N b_n \sin\left(\frac{n\pi t}{L}\right) \tag{12}$$

forming the column vectors,

$$\vec{\beta}^T = \begin{bmatrix} a_0 \\ a_1 \\ \vdots \\ a_N \\ b_1 \\ \vdots \\ b_N \end{bmatrix}, \vec{X} = \begin{bmatrix} 1 \\ \cos\left(\frac{\pi t}{L}\right) \\ \vdots \\ \cos\left(\frac{N\pi t}{L}\right) \\ \sin\left(\frac{\pi t}{L}\right) \\ \vdots \\ \sin\left(\frac{N\pi t}{L}\right) \end{bmatrix} \tag{13}$$

and adding an error term, the Fourier series expansion takes the form of the standard linear model:

$$y(t) = \vec{\beta}^T \vec{X} + \varepsilon(t) \tag{14}$$

With the column vector \vec{X} of cosines and sines of harmonic frequencies of $y(t)$, the Fourier coefficients can therefore be estimated using ordinary least squares,

$$\vec{\beta}_{OLS} = (\vec{X}^T \vec{X})^{-1} \vec{X}^T y(t) \tag{15}$$

With the further assumption of normal i.i.d. errors, this approach allows the full machinery of regression to be brought to bear on the calculation of Fourier coefficients, including t -statistics for coefficient discernibility, F -statistics for hypothesis testing, and R^2 for model selection. For example, the variance-covariance matrix of the OSL estimator is

$$E\left[(\vec{\beta}_{OLS} - \vec{\beta})(\vec{\beta}_{OLS} - \vec{\beta})^T\right] \approx \frac{(y - X\vec{\beta}_{OLS})^T (y - X\vec{\beta}_{OLS})}{n - k} (\vec{X}^T \vec{X})^{-1} \tag{16}$$

and the standard errors of the estimates are the square roots of the diagonal elements of this matrix. The spectrum is given by the sum of squares of Fourier sine and cosine coefficients,

$$S_i = a_i^2 + b_i^2 \tag{17}$$

for each harmonic frequency i . The standard error of the energy at each frequency is then given by the square root of the variance of the spectrum, approximated by first-order Taylor expansion, assuming zero covariances as expected from orthogonal regressors,

$$Var(a_i^2 + b_i^2) \approx 4[Var(a_i) + Var(b_i)] \tag{18}$$

3. References

- Petit, J.R.; Jouzel, J.; Raynaud, D.; Barkov, N.I.; Barnola, J.M.; Basile, I.; Bender, M.; Chappellaz, J.; Davis, J.; Delaygue, G.; et al. Climate and atmospheric history of the past 420,000 years from the Vostok ice core, Antarctica. *Nature* **1999**, *399*, 429–436, doi:10.1038/20859.
- Petit, J.R.; Jouzel, J.; Raynaud, D.; Barkov, N.I.; Barnola, J.M.; Basile, I.; Bender, M.; Chappellaz, J.; Davis, J.; Delaygue, G.; et al. Vostok ice core data for 420,000 years. 2001; IGBP PAGES/World Data Center for Paleoclimatology Data Contribution Series #2001-076. NOAA/NGDC Paleoclimatology Program, Boulder TOC, USA.
- Lüthi, D.; Floch, M.L.; Bereiter, B.; Blunier, T.; Barnola, J.-M.; Siegenthaler, U.; Raynaud, D.; Jouzel, J.; Fischer, H.; Kawamura, K.; Stocker, T.F. High-resolution carbon dioxide concentration record 648,000–800,000 years before present. *Nature* **2008**, *453*, 379–382, doi:10.1038/nature06949.
- Veres, D.; Bazin, L.; Landais, A.; Kele, T.H.M.; Lemieux-Dudon, B.; Parrenin, F.; Martinerie, P.; Blayo, E.; Blunier, T.; Capron, E.; et al. The Antarctic ice core chronology (AICC2012): an optimized multi-parameter and multi-site dating approach for the last 120 thousand years. *Clim. Past* **2013**, *9*, 1733–1748, doi:10.5194/gmd-8-1473-2015.
- Bazin, L.; Landais, A.; Lemieux-Dudon, B.; Kele, H.T.M.; Veres, D.; Parrenin, F.; Martinerie, P.; Ritz, C.; Capron, E.; Lipenkov, V.; et al. An optimized multi-proxy, multi-site Antarctic ice and gas orbital chronology (AICC2012): 120–800 ka. *Clim. Past* **2013**, *9*, 1715–1731, doi: org/10.5194/cp-9-1715-2013.
- <http://www.ncdc.noaa.gov/data-access/paleoclimatology-data/datasets>.
- Huybers, P. Early Pleistocene glacial cycles and the integrated summer insolation forcing. *Science* **2006**, *313*, 508–511, doi:10.1126/science.1125249.
- Lorius, C.; Ritz, C.; Jouzel, J.; Merlivat, L.; Barkov, N.I. A 150,000-year climatic record from Antarctic ice. *Nature* **1985**, *316*, 591–596, doi:10.1038/316591a0.
- Jouzel, J.; Lorius, C.; Petit, J.R.; Genthon, C.; Barkov, N.I.; Kotlyakov, V.M.; Petrov, V.M. Vostok ice core: a continuous isotope temperature record over the last climatic cycle (160 000 years). *Nature* **1987**, *329*, 402–408, doi:10.1038/329403a0.
- Jouzel, J.; Barkov, N.I.; Barnola, J.M.; Bender, M.; Chappellaz, J.; Genthon, C.; Kotlyakov, V.M.; Lipenkov, V.; Lorius, C.; Petit, J.R.; Raynaud, D.; Raisbeck, G.; Ritz, C.; Sowers, T.; Stievenard, M.; Yiou, F.; Yiou, P. Extending the Vostok ice-core record of paleoclimate to the penultimate glacial period. *Nature* **1993**, *364*, 407–412, doi:10.1038/364407a0.
- Jouzel, J.; Waelbroeck, C.; Malaize, B.; Bender, M.; Petit, J.R.; Stievenard, M.; Barkov, N.I.; Barnola, J.M.; King, T.; Kotlyakov, V.M.; Lipenkov, V.; Lorius, C.; Raunaud, D.; Ritz, C.; Sowers, T. Climate interpretation of the recently extended Vostok ice records. *Clim. Dynam.* **1996**, *12*, 513–521, doi:org/10.1007/BF00207935.
- Wunsch, C. Quantitative estimate of the Milankovitch-forced contribution to observed Quaternary climate change. *Quat. Sci. Rev.* **2004**, *23*, 101–112, doi:10.1016/j.quascirev.2004.02.014.
- Nyquist, H. Certain topics in telegraph transmission theory. *AIEE* **1928**; *47*, 617–644. reprinted as a Classic Paper in *Trans. IEEE* **2002**, *90*, 280–305, doi:10.1109/T-AIEE.1928.5055024.
- Shannon, C.E. Communication in the presence of noise. *Proc IRE* **1949**, *37*, 10–21, reprinted as a Classic Paper in *Proc. IRE* **1998**, *86*, 447–457, doi:10.1109/JRPROC.1949.232969.
- Landau, H.J. Necessary density conditions for sampling and interpolation of certain entire functions. *Acta Math.* **1967**, *117*, 37–52, doi:10.1007/BF02395039.
- Luo, F.; Hong, Y.; Rashid, M.H. *Digital Power Electronics and Applications*. Academic Press: New York, USA, 2005, 464 pp., ISBN 0080459021, 9780080459028.
- Pisias, N.G.; Mix, A.C. Aliasing of the geologic record and the search for long-period Milankovitch cycles. *Paleoceanog.* **1988**, *3*, 613–619, doi: 10.1029/PA003i005p00613.
- Yiou, F.; Raisbeck, G.M.; Baumgartner, S.; Beer, J.; Hammer, C.; Johnsen, S.; Jouzel, J.; Kubik, P.W.; Lestringuez, J.; Stievenard, M.; Suter, M.; Yiou, P. Beryllium 10 in the Greenland Ice Core Project ice core at Summit, Greenland. *J. Geophys. Res.* **1997**, *102*, 26,783–26,794, doi:10.1029/97JC01265.
- Gille, S.T.; Hughes, C.W. Aliasing of high-frequency variability by altimetry: Evaluation from bottom pressure recorders. *Geophys. Res. Lett.* **2001**, *28*, 1755–1758, doi:10.1029/2000GL012244.

20. Madden, R.A.; Jones, R.H. A quantitative estimate of the effect of aliasing in climatological time series. *J. Clim.* **2001**, *14*, 3987–3993. doi: org/10.1175/1520-0442(2001)014<3987:AQEOTE>2.0.CO;2.
21. Meeker, L.D.; Mayewski, P.A.; Grootes, P.M.; Alley, R.B.; Bond, G.C. Comment on "On sharp spectral lines in the climate record and the millennial peak" by Carl Wunsch. *Paleoceanog.* **2001**, *16*, 544–547, doi: 10.1029/2000PA000607.
22. Wunsch, C. On sharp spectral lines in the climate record and the millennial peak. *Paleoceanog.* **2000**, *15*, 417–424, doi:10.1029/1999PA000468.
23. Wunsch, C. Reply. *Paleoceanog.* **2001**, *16*, 548, doi: 10.1029/2000PA000618.
24. Wunsch, C.; Gunn, D.E. A densely sampled core and climate variable aliasing. *Geo-Mar. Lett.* **2003**, *23*, 64–71, doi:org/10.1007/s00367-003-0125-2.
25. Mudelsee, M. *Climate Time Series Analysis: Classical Statistical and Bootstrap Methods*, 2nd. ed.; Springer: New York, USA, 2014, doi.org/10.1007/978-3-319, Print ISBN 978-3-319-04449-1, Online ISBN 978-3-319-04450-7.
26. Jerri, A.J. The Shannon Sampling Theorem—Its various extensions and applications: A tutorial review. *Proc. IEEE* **1977**, *65*, 1565–1596, doi:10.1109/PROC.1977.10771.
27. Pedro, J.B.; van Ommen, T.D.; Rasmussen, S.O.; Morgan, V.L.; Chappellaz, J.; Moy, A.D.; Masson-Delmotte, V.; Delmotte, M. The last deglaciation: timing the bipolar seesaw. *Clim. Past* **2011a**, *7*, 671–683, doi:org/10.5194/cp-7-671-2011.
28. Parrenin, F.; Jouzel, J.; Waelbroeck, C.; Ritz, C.; Barnola, J.-M. Dating the Vostok ice core by an inverse method. *J. Geophys. Res.* **2001**, *106*, 31837–31851, doi:10.1029/2001JD900245.
29. Ruddiman, W.F.; Raymo, M.E. A methane-based time scale for Vostok ice. *Quat. Sci. Rev.* **2003**, *22*, 141–155, doi:org/10.1016/S0277-3791(02)00082-3.
30. Bender, M.L.; Floch, G.; Chappellaz, J.; Suwa, M.; Barnola, J.-M.; Blunier, T.; Dreyfus, G.; Jouzel, J.; Parrenin, F. Gas age–ice age differences and the chronology of the Vostok ice core, 0–100 ka. *J. Geophys. Res.* **2006**, *111*, D21115, doi:10.1029/2005JD006488.
31. Jouzel, J.; Masson-Delmotte, V.; Cattani, O.; Dreyfus, G.; Falourd, S.; Hoffmann, G.; Minster, B.; Nouet, J.; Barnola, J.M.; Chappellaz, J.; et al. Orbital and millennial Antarctic climate variability over the past 800,000 years. *Science* **2007**, *317*, 793–797, doi:10.1126/science.1141038.
32. Masson, V.; Vimeux, F.; Jouzel, J.; Morgan, V.; Delmotte, M.; Ciais, P.; Hammer, C.; Johnsen, C.; Lipenkov, V.Y.; Mosley-Thompson, E.; Petit, J.R.; Steig, E.J.; Stievenard, M.; Vaikmae, R. Holocene climate variability in Antarctica based on 11 ice-core isotopic records. *Quat. Res.* **2000**, *54*, 348–358, doi: 10.1006/qres.2000.2172.
33. Johnsen, S. J.; Clausen, H.B.; Cuffey, K.M.; Hoffmann, G.; Schwander, J.; Creyts, T. Diffusion of stable isotopes in polar firn and ice: The isotope effect in firn diffusion. In: *Physics of Ice Core Records*, Editor, Hondoh, T. Hokkaido University Press: Sapporo, Japan, 2000, pp.121–140, no ISBN.
34. Münch, T.; Kipfstuhl, S.; Freitag, J.; Meyer, H.; Laepple, T. Regional climate signal vs. local noise: a two-dimensional view of water isotopes in Antarctic firn at Kohlen station, Dronning Maud Land. *Clim. Past Discuss.* **2016**, *11*, 5605–5649, doi:10.5194/cp-12-1565-2016.
35. Oerter, H.; Wilhelms, F.; Jung-Rothenhausler, F.; Göktas, F.; Miller, H.; Graf, W.; Sommer, S. Accumulation rates in Dronning Maud Land, Antarctica, as revealed by dielectric-profiling measurements of shallow firn cores. *Ann. Glaciol.* **2000**, *30*, 27–34, doi:10.3189/172756400781820705.
36. Steen-Larsen, H.C.; Masson-Delmotte, V.; Sjolte, J.; Johnsen, S.J.; Vinther, B.M.; Bréon, F.-M.; Clausen, H.B.; Dahl-Jensen, D.; Falourd, S.; Fettweis, X.; Gallée, H.; Jouzel, J.; Kageyama, M.; Lerche, H.; Minster, B.; Picard, G.; Punge, H.J.; Ris, C.; Salas, D.; Schwander, J.; Steen, K.; Sveinbjörnsdóttir, A.E.; Svensson, A.; White, J. Understanding the climatic signal in the water stable isotope records from the NEEM shallow firn/ice cores in northwest Greenland. *J. Geophys. Res.* **2011**, *116*, D06108, doi:10.1029/2010JD014311.
37. van den Broeke, M. Depth and density of the Antarctic firn layer. *Arct. Antarct. Alpine Res.* **2008**, *40*, 432–438, doi:10.1657/1523-0430(07-021)[BROEKE]2.0.CO;2.
38. Ekaykin, A.A.; Lipenkov, V.-Y.; Barkov, N.I.; Petit, J.R.; Masson-Delmotte, V. Spatial and temporal variability in isotope composition of recent snow in the vicinity of Vostok station, Antarctica: implications for ice-core record interpretation. *Ann. Glaciol.* **2002**, *35*, 181–186, doi-org.oca.ucsc.edu/10.3189/172756402781816726.

39. Ekaykin, A.A.; Kozachek, A.V.; Lipenkov, V.-Y.; Shibaev, Y.A. Multiple climate shifts in the southern hemisphere over the past three centuries based on central Antarctic snow pits and core studies. *Ann. Glaciol.* **2012**, *55*, 259-266, doi:org/10.3189/172756402781816726..
40. Sommer, S.; Appenzeller, C.; Röthlisberger, R.; Hutterli, M.A.; Stauer, B.; Wagenbach, D.; Oerter, H.; Wilhelms, F.; Miller, H.; Mulvaney, R. Glacio-chemical study spanning the last 2 kyr on three ice cores from Dronning Maud Land, Antarctica: 1. Annually resolved accumulation rates. *J. Geophys. Res.* **2000**, *105*, 29411–29421, doi:10.1029/2000JD900450.
41. Blunier, T.; Brook, E.J. Timing of millennial-scale climate change in Antarctica and Greenland during the last glacial period. *Science* **2001**, *291*, 109-112, doi:10.1126/science.291.5501.109.
42. EPICA Community Members. One-to-one coupling of glacial climate variability in Greenland and Antarctica. *Nature* **2006**, *444*, 195-198, doi:10.1038/nature05301.
43. Huybers, P. Combined obliquity and precession pacing of late Pleistocene deglaciations. *Nature* **2011**, *480*, 229-232, doi:10.1038/nature10626.

4.SM Table 1. Datapoints corresponding to all peaks and troughs of each of the 650 TO_{C350V} cycles identified and analyzed in this study.

TO _{C350V} count	TO _{C350V} number	End time (yb1950)	ΔT at end (°C)	# cooling datapoints	Peak time (yb1950)	Peak ΔT (°C)	# warming datapoints	Start time (yb1950)	Start ΔT (°C)	Interpolated CO ₂ at peak (ppmv)
1	1	149	-0.81	3	190	0.36	3	234	-1.84	284.7 (280.4)
2	2	234	-1.84	4	304	0.22	3	351	-0.75	284.7 (274.9)
3	3	351	-0.75	3	397	1.33	2	420	0.35	284.7 (279)
4	3a	420	0.35	2	444	0.18	3	552	-1.61	
5	4	552	-1.61	4	637	-0.02	4	726	-1.54	284.7 (281.3)
6	5	726	-1.54	3	788	-0.17	3	881	-0.78	284.7 (280)
7	6	881	-0.78	2	912	-0.17	2	944	-0.25	284.7 (278.4)
8	6a	944	-0.25	2	976	-0.28	2	1,009	-0.81	
9	7	1,009	-0.81	3	1074	-0.27	2	1,107	-0.83	284.7 (279.1)
10	8	1,107	-0.83	3	1176	-0.27	4	1,285	-1.64	284.7 (277.7)
11	9	1,285	-1.64	3	1356	0.33	3	1,426	-0.13	284.7 (277.4)
12	10	1,246	-0.13	2	1,461	-0.03	3	1,535	-1.00	284.7 (279.1)
13	11	1,535	-1.00	2	1,573	-0.96	3	1,652	-1.51	284.7 (280)
14	12	1,652	-1.51	2	1,692	-0.88	4	1,812	-1.24	284.7 (278.9)
15	13	1,812	-1.24	4	1,931	0.15	7	2,009	-0.45	284.7 (276.9)
16	14	2,009	-0.45	2	2,049	-0.38	4	2,089	-0.53	284.7 (276.7)
17	14a	2,089	-0.53	2	2,129	-0.61	2	2,171	-0.95	
18	15	2,171	-0.95	4	2,291	1.16	3	2,374	-1.44	284.7 (278)
19	15a	2,374	-1.44	2	2,418	-0.73	2	2,460	-0.63	
20	16	2,460	-0.63	2	2,501	0.3	3	2,585	-1.36	283.4 (276)
21	16a	2,585	-1.36	2	2,628	-0.17	2	2,670	-0.02	
22	17	2,628	-0.17	3	2,670	-0.02	3	2,760	-1.97	282.0 (275)
23	18	2,760	-1.97	3	2,847	0.58	4	2,980	-1.41	280.0 (275.3)
24	19	2,980	-1.41	3	3,070	-0.25	2	3,114	-0.53	278.2 (276)
25	20	3,114	-0.53	3	3,201	0.15	3	3,289	-0.61	277.0 (274)
26	20a	3,289	-0.61	2	3,334	-0.30	2	3,379	-0.13	
27	21	3,379	-0.13	2	3,422	0.22	3	3,511	-0.91	274.5 (274)
28	22	3,511	-0.91	4	3,646	0.65	4	3,778	-0.63	272.8 (272)
29	23	3,778	-0.63	3	3,870	0	5	4,057	-0.75	268.0
30	23a	4,009	-0.73	3	4,057	-0.75	3	4,153	-1.09	
31	24	4,153	-1.09	7	4,423	1.13	6	4,690	-0.88	267.2
32	24a	4,690	1.13	2	4,552	0.88	3	4,690	-0.88	
33	25	4,690	-0.88	3	4,786	0.25	3	4,880	-1.14	266.5
34	26	4,880	-1.14	3	4,977	-0.36	2	5,025	-0.66	266.1
35	27	5,025	-0.66	3	5,118	0.18	2	5,165	-0.38	265.7
36	28	5,165	-0.38	3	5,259	0.28	3	5,351	0.08	265.0
37	29	5,351	0.08	2	5,420	0.50	3	5,534	0.02	264.2

38	30	5,534	0.02	2	5,581	0.08	5	5,769	-0.25	264.0
39	31	5,769	-0.25	3	5,909	0.45	3	6,004	-0.73	263.0
40	32	6,004	-0.73	3	6,099	0.32	3	6,193	-0.33	262.3
41	33	6,193	-0.33	3	6,287	0.28	3	6,385	-1.59	262.1
42	34	6,385	-1.59	3	6,486	-0.31	3	6,583	-0.65	260.7
43	35	6,583	-0.65	2	6,654	0.37	4	6,823	-1.28	259.5
44	36	6,823	-1.28	3	6,924	-0.58	4	7,074	-1.20	257.7
45	37	7,074	-1.20	3	7,172	0.02	5	7,364	-0.81	255.7
46	37a	7,267	-0.11	2	7,315	-0.29	2	7,364	-0.81	
47	38	7,364	-0.81	3	7,462	0.02	2	7,509	-0.03	255.0
48	39	7,509	-0.03	2	7,555	0.48	2	7,602	-0.02	257.1
49	39a	7,602	-0.02	2	7,649	0.02	3	7,745	-0.72	257.5
50	40	7,745	-0.72	2	7,794	-0.57	3	7,894	-0.93	258.5
51	41	7,894	-0.93	3	7,994	-0.54	2	8,043	-0.64	260.0
52	42	8,043	-0.64	3	8,135	2.06	3	8,226	-0.87	259.6
53	43	8,226	-0.87	4	8,374	-0.21	6	8,619	-0.73	259.9
54	44	8,619	-0.73	3	8,716	0.34	6	8,811	-0.81	260.0
55	45	8,811	-0.81	2	8,861	-0.53	3	8,960	-0.88	260.05
56	46	8,960	-0.88	3	9,058	-0.41	2	9,107	-0.6	260.1
57	47	9,107	-0.60	4	9,252	0.26	4	9,396	-0.82	260.2
58	47a	9,396	-0.82	3	9,494	-0.16	2	9,542	-0.16	
59	48	9,542	-0.16	3	9,635	0.51	4	9,782	-0.85	260.6
60	49	9,782	-0.85	3	9,881	-0.36	3	9,978	-0.65	261.1
61	50	9,978	-0.65	2	10,027	-0.28	3	10,124	-0.58	261.4
62	51	10,124	-0.58	3	10,218	0.52	3	10,315	-1.3	261.9
63	52	10,315	-1.30	3	10,415	-0.43	4	10,515	-0.77	262.4
64	52a	10,515	-0.77	2	10,564	-0.79	3	10,655	-0.96	
65	53	10,655	-0.96	3	10,764	-0.26	3	10,861	-0.62	263.0
66	54	10,861	-0.62	3	10,957	-0.12	2	11,005	-0.23	263.5
67	54a	11,005	-0.23	2	11,053	0.02	2	11,100	0.09	
68	55	11,100	0.09	3	11,191	0.81	3	11,286	-0.48	252.7
69	56	11,286	-0.48	2	11,334	-0.27	3	11,434	-1.22	244.8
70	56a	11,434	-1.22	2	11,485	-1.29	2	11,590	-1.59	
71	56b	11,590	-1.59	2	11,642	-1.61	3	11,749	-2.20	
72	56c	11,749	-2.20	2	11,805	-2.37	2	11,861	-2.85	
73	57	11,861	-2.85	3	11,973	-2.19	3	12,087	-3.09	237.1
74	58	12,087	-3.09	2	12,144	-2.77	2	12,202	-2.90	237.9
75	58a	12,144	-2.77	2	12,202	-2.90	3	12,323	-4.18	

76	59	12,323	-4.18	3	12,446	-3.61	4	12,507	-3.76	237.4
77	59a	12,446	-3.61	2	12,507	-3.76	3	12,632	-4.25	
78	60	12,632	-4.25	4	12,815	-3.24	5	12,874	-3.40	237.2
79	60a	12,874	-3.40	2	12,934	-3.50	3	13,055	-3.85	
80	60b	13,055	-3.85	2	13,116	-3.75	2	13,177	-3.72	
81	61	13,177	-3.72	3	13,296	-3.17	2	13,355	-3.17	236.3
82	61a	13,296	-3.17	2	13,355	-3.17	3	13,476	-4.28	
83	61b	13,476	-4.28	3	13,600	-3.57	2	13,659	-3.27	228.0
84	62	13,718	-2.91	3	13,828	-2.04	2	13,883	-2.24	
85	63	13,883	-2.24	2	13,938	-2.06	9	14,404	-4.11	226.5
86	64	14,404	-4.11	2	14,466	-3.64	3	14,589	-4.34	218.0
87	65	14,589	-4.34	3	14,713	-3.92	2	14,775	-4.14	216.0
88	65a	14,713	-3.92	2	14,775	-4.14	3	14,904	-4.68	
89	66	14,904	-4.68	2	14,968	-4.44	2	15,032	-4.66	212.0
90	66a	14,968	-4.44	2	15,032	-4.66	3	15,167	-5.40	
91	66b	15,167	-5.40	2	15,234	-5.00	2	15,300	-4.81	
92	67	15,300	-4.81	2	15,366	-4.74	3	15,501	-5.71	207.0
93	68	15,501	-5.71	3	15,639	-5.00	2	15,708	-5.57	204.0
94	69	15,708	-5.57	2	15,777	-5.29	3	15,915	-6.19	202.7
95	70	15,915	-6.19	3	16,057	-5.75	2	16,128	-6.08	199.0
96	70a	16,128	-6.08	2	16,201	-6.34	4	16,350	-6.88	
97	71	16,350	-6.88	3	16,502	-6.74	3	16,653	-6.97	193.5
98	71a	16,653	-6.97	2	16,729	-7.16	4	16,974	-8.51	
99	71b	16,974	-8.51	3	17,139	-7.60	3	17,219	-7.53	
100	72	16,974	-8.51	5	17,298	-7.45	3	17,462	-8.27	186.0
101	73	17,462	-8.27	2	17,544	-7.68	3	17,706	-7.84	183.2
102	74	17,706	-7.84	3	17,868	-7.72	4	18,116	-8.63	182.4
103	74a	17,848	-8.63	2	17,949	-8.16	2	18,283	-7.89	
104	74b	18,365	-7.74	3	18,283	-7.89	2	18,365	-8.63	
105	75	18,283	-7.89	2	18,365	-7.74	3	18,530	-8.50	184.0
106	75a	18,530	-8.50	2	18,615	-8.43	2	18,701	-8.73	184.9
107	76	18,701	-8.73	3	18,870	-7.58	2	18,950	-7.63	185.5
108	76a	18,870	-7.58	2	18,950	-7.63	3	19,116	-8.26	
109	77	19,116	-8.26	4	19,362	-7.54	2	19,443	-7.70	186.8
110	77a	19,362	-7.54	2	19,443	-7.70	4	19,696	-8.71	
111	77b	19,696	-8.71	2	19,782	-8.52	2	19,868	-8.61	188.4
112	77c	19,868	-8.61	2	19,953	-7.99	2	20,035	-7.62	
113	78	19,953	-7.99	2	20,035	-7.62	2	20,116	-7.84	189.3

114	79	20,116	-7.84	2	20,197	-7.52	3	20,361	-8.11	180.4
115	79a	20,361	-8.11	3	20,528	-8.03	2	20,611	-8.04	189.6
116	80	20,611	-8.04	3	20,777	-7.87	3	20,943	-8.12	189.8
117	81	20,943	-8.12	4	21,192	-7.91	4	21,442	-8.09	190.0
118	82	21,442	-8.09	3	21,605	-7.36	4	21,854	-8.33	190.2
119	83	21,854	-8.33	2	21,939	-8.12	4	22,240	-8.82	190.4
120	84	22,240	-8.82	3	22,457	-8.30	5	22,803	-8.59	191.1
121	85	22,803	-8.59	3	22,972	-7.92	5	23,324	-9.01	191.6
122	86	23,324	-9.01	3	23,497	-7.76	3	23,755	-8.63	190.7
123	87	23,755	-8.63	6	24,186	-7.87	3	24,363	-9.39	190.2
124	87a	24,363	-9.39	3	24,537	-7.53	2	24,619	-7.51	
125	88	24,619	-7.51	4	24,860	-7.00	3	25,024	-8.14	190.0
126	89	25,024	-8.14	4	25,277	-7.68	3	25,445	-8.57	189.6
127	90	25,445	-8.57	4	25,776	-6.98	2	25,855	-7.26	189.3
128	90a	25,855	-7.26	2	25,936	-7.29	3	26,099	-7.48	
129	91	26,099	-7.48	2	26,180	-7.16	7	26,681	-8.09	188.9
130	92	26,681	-8.09	3	26,849	-7.56	4	27,156	-9.02	190.0
131	93	27,156	-9.02	5	27,555	-7.84	3	27,730	-8.66	193.5
132	94	27,730	-8.66	7	28,247	-7.49	3	28,420	-8.82	195.5
133	95	28,420	-8.82	7	28,967	-6.71	8	29,594	-8.37	197.0
134	95a	29,594	-8.37	2	29,682	-8.33	2	29,771	-8.58	199.8
135	96	29,771	-8.58	6	30,201	-7.02	3	30,368	-7.83	201.2
136	97	30,368	-7.83	6	30,788	-7.30	5	31,130	-8.05	203.5
137	98	31,130	-8.05	3	31,302	-7.65	2	31,560	-8.20	204.9
138	98a	31,560	-8.20	3	31,733	-7.40	2	31,815	-7.14	
139	99	31,815	-7.14	3	31,976	-6.74	4	32,219	-7.27	206.0
140	100	32,219	-7.27	2	32,300	-6.61	3	32,463	-7.49	207.0
141	101	32,463	-7.49	3	32,626	-6.62	3	32,829	-7.47	207.25
142	102	32,829	-7.47	2	32,955	-7.29	4	33,209	-7.60	207.9
143	103	33,209	-7.60	3	33,376	-7.07	3	33,544	-7.54	208.6
144	104	33,544	-7.54	3	33,711	-7.12	3	33,877	-7.36	208.9
145	105	33,877	-7.36	3	34,041	-6.53	2	34,121	-6.88	209.1
146	106	34,121	-6.88	3	34,281	-6.25	2	34,360	-6.59	209.1
147	107	34,360	-6.59	3	34,515	-6.01	2	34,592	-6.15	209.1
148	107a	34,592	-6.15	2	34,669	-5.87	2	34,744	-5.70	
149	108	34,744	-5.70	3	34,889	-4.82	4	35,108	-5.98	209.1
150	109	35,108	-5.98	4	35,409	-5.24	4	35,631	-5.65	209.1
151	110	35,631	-5.65	2	35,705	-5.41	3	35,855	-5.72	209.1

152	110a	35,855	-5.72	2	35,930	-5.77	2	36,007	-6.22	
153	110b	36,007	-6.22	2	36,086	-6.40	3	36,248	-7.03	
154	110c	36,248	-7.03	2	36,331	-7.22	2	36,416	-7.70	
155	111	36,416	-7.70	3	36,585	-6.67	2	36,666	-6.97	209.1
156	112	36,666	-6.97	3	36,827	-6.02	5	37,148	-6.90	209.1
157	112a	37,148	-6.90	2	37,230	-6.90	3	37,396	-7.20	
158	113	37,396	-7.20	3	37,558	-5.97	3	37,718	-6.88	209.1
159	114	37,718	-6.88	4	37,959	-6.30	6	38,493	-7.18	209.1
160	114a	38,493	-7.18	3	38,702	-6.73	2	38,783	-6.69	
161	115	38,783	-6.69	6	39,224	-5.93	3	39,460	-6.24	209.1
162	115a	39,460	-6.24	2	39,579	-6.13	2	39,657	-6.13	
163	116	39,657	-6.13	3	39,812	-5.48	3	39,971	-6.96	209.1
164	116a	39,971	-6.96	2	40,054	-6.91	2	40,138	-7.21	208.9
165	117	40,138	-7.21	3	40,305	-6.31	3	40,468	-6.91	208.2
166	118	40,468	-6.91	3	40,632	-6.56	2	40,714	-6.67	207.0
167	119	40,714	-6.67	3	40,914	-5.74	3	41,112	-6.59	205.0
168	120	41,112	-6.59	5	41,415	-5.02	3	41,564	-5.48	203.0
169	121	41,564	-5.48	3	41,710	-4.53	2	41,782	-5.08	202.0
170	122	41,782	-5.08	3	41,927	-4.68	3	42,077	-5.69	200.4
171	123	42,077	-5.69	3	42,225	-4.65	3	42,374	-5.70	199.6
172	124	42,374	-5.70	2	42,451	-5.40	2	42,527	-5.49	198.9
173	125	42,527	-5.49	2	42,603	-5.43	3	42,758	-6.13	198.0
174	126	42,758	-6.13	3	42,916	-5.88	2	42,994	-5.93	196.5
175	127	42,994	-5.93	4	43,226	-5.50	3	43,385	-6.45	195.5
176	128	43,385	-6.45	2	43,464	-5.42	3	43,619	-6.68	194.4
177	129	43,619	-6.68	3	43,785	-6.48	2	43,868	-6.94	192.4
178	130	43,868	-6.94	3	44,036	-6.72	3	44,206	-7.27	191.5
179	131	44,206	-7.27	2	44,292	-6.94	3	44,463	-7.51	190.8
180	132	44,463	-7.51	3	44,634	-6.15	3	44,800	-7.44	189.8
181	133	44,800	-7.44	3	44,972	-6.68	2	45,055	-6.72	189.2
182	134	45,055	-6.72	2	45,139	-6.69	3	45,315	-8.16	189.1
183	135	45,315	-8.16	3	45,495	-7.64	2	45,587	-7.94	188.9
184	136	45,587	-7.94	3	45,762	-6.55	3	45,932	-7.01	188.5
185	136a	45,932	-7.01	2	46,018	-7.02	5	46,370	-7.51	
186	137	46,370	-7.51	3	46,543	-6.78	3	46,713	-6.91	188.8
187	138	46,713	-6.91	2	46,797	-6.48	3	46,966	-6.92	188.5
188	139	46,966	-6.92	4	47,214	-5.92	3	47,378	-6.73	191.5
189	140	47,378	-6.73	2	47,462	-6.55	3	47,631	-6.99	196.2

190	141	47,631	-6.99	3	47,798	-6.28	3	47,966	-6.85	202.2
191	142	47,966	-6.85	2	48,050	-6.46	2	48,134	-6.65	207.4
192	143	48,134	-6.65	3	48,300	-6.02	2	48,381	-6.05	210.2
193	144	48,381	-6.05	2	48,461	-5.80	5	48,787	-6.48	211.0
194	145	48,787	-6.48	4	49,034	-5.76	3	49,193	-5.89	213.0
195	146	49,193	-5.89	2	49,311	-5.51	4	49,591	-6.07	215.2
196	147	49,591	-6.07	3	49,750	-5.30	3	49,907	-5.60	212.0
197	148	49,907	-5.60	3	50,061	-5.03	3	50,217	-5.70	206.4
198	149	50,217	-5.70	2	50,295	-5.37	2	50,374	-5.54	203.0
199	149a	50,374	-5.54	2	50,452	-5.54	2	50,531	-5.65	
200	150	50,531	-5.65	3	50,688	-5.19	3	50,847	-6.07	197.2
201	150a	50,847	-6.07	2	50,928	-5.89	2	51,009	-5.74	
202	151	51,009	-5.74	3	51,159	-3.77	3	51,306	-5.38	190.4
203	151a	51,306	-5.38	2	51,384	-5.60	2	51,549	-6.60	
204	152	51,549	-6.60	3	51,715	-5.47	3	51,874	-6.02	192.8
205	153	51,874	-6.02	2	51,995	-5.56	3	52,195	-5.84	194.3
206	154	52,195	-5.84	3	52,352	-5.03	3	52,511	-6.13	196.5
207	154a	52,511	-6.13	2	52,594	-6.23	2	52,679	-6.71	
208	155	52,679	-6.71	3	52,846	-6.10	3	53,019	-7.18	199.5
209	156	53,019	-7.18	5	53,355	-5.55	3	53,563	-6.65	201.5
210	157	53,563	-6.65	4	53,775	-6.04	3	53,942	-6.49	204.0
211	158	53,942	-6.49	2	54,026	-6.14	3	54,198	-7.06	205.2
212	159	54,198	-7.06	3	54,372	-6.40	3	54,544	-6.80	207.0
213	160	54,544	-6.80	2	54,629	-6.17	2	54,713	-6.35	208.0
214	160a	54,713	-6.35	2	54,797	-6.29	3	54,967	-6.71	209.2
215	160b	54,967	-6.71	2	55,052	-6.31	2	55,136	-6.16	
216	161	55,136	-6.16	3	55,297	-5.34	2	55,377	-5.65	211.5
217	162	55,377	-5.65	3	55,536	-5.21	2	55,615	-5.43	213.0
218	162a	55,615	-5.43	2	55,694	-5.54	2	55,775	-5.81	
219	163	55,775	-5.81	3	55,933	-4.80	2	56,009	-5.09	215.2
220	164	56,009	-5.09	3	56,163	-4.71	3	56,317	-5.11	217.0
221	165	56,317	-5.11	2	56,394	-4.76	3	56,548	-5.10	218.0
222	166	56,548	-5.10	2	56,624	-4.35	3	56,774	-4.88	219.5
223	167	56,774	-4.88	4	56,993	-3.68	4	57,215	-4.73	221.2
224	168	57,215	-4.73	2	57,289	-4.01	4	57,475	-4.85	218.2
225	168a	57,475	-4.85	2	57,590	-4.86	2	57,669	-5.78	
226	169	57,669	-5.78	3	57,828	-4.65	2	57,905	-4.98	210.4
227	170	57,905	-4.98	3	58,057	-4.62	3	58,211	-4.96	209.8

228	171	58,211	-4.96	3	58,360	-4.22	2	58,436	-4.93	209.0
229	171a	58,436	-4.93	2	58,514	-5.21	4	58,759	-6.06	
230	172	58,759	-6.06	3	58,925	-5.85	3	59,093	-6.41	208.0
231	173	59,093	-6.41	4	59,345	-5.85	2	59,428	-6.03	206.5
232	174	59,428	-6.03	4	59,674	-5.53	4	60,007	-6.53	205.5
233	175	60,007	-6.53	3	60,177	-6.11	3	60,348	-6.45	203.8
234	176	60,348	-6.45	3	60,519	-6.28	3	60,692	-6.58	202.8
235	176a	60,692	-6.58	2	60,779	-6.61	3	60,961	-7.48	
236	176b	60,961	-7.48	2	61,052	-6.98	2	61,141	-6.81	
237	177	61,141	-6.81	2	61,229	-6.53	2	61,317	-6.88	201.8
238	178	61,317	-6.88	2	61,406	-6.86	3	61,586	-7.26	200.5
239	179	61,586	-7.26	3	61,765	-6.50	4	62,031	-7.10	200.0
240	180	62,031	-7.10	2	62,121	-7.05	3	62,307	-7.72	199.1
241	181	62,307	-7.72	2	62,401	-7.64	4	62,497	-8.09	197.9
242	181a	62,783	-7.54	2	62,877	-7.51	4	63,157	-7.51	
243	182	63,157	-7.51	4	63,424	-6.26	2	63,512	-6.84	196.3
244	183	63,512	-6.84	3	63,688	-6.41	2	63,776	-6.83	195.4
245	184	63,776	-6.83	3	63,954	-6.79	4	64,228	-7.70	194.9
246	185	64,228	-7.70	3	64,416	-7.40	2	64,510	-7.91	193.2
247	186	64,510	-7.91	2	64,605	-7.43	3	64,793	-7.97	193.0
248	186a	64,793	-7.97	2	64,890	-7.92	2	64,987	-8.17	192.5
249	186b	64,987	-8.17	2	65,085	-7.98	2	65,182	-7.95	
250	187	65,182	-7.95	3	65,371	-7.25	2	65,756	-8.85	191.6
251	187a	65,464	-7.49	2	65,559	-7.71	3	65,756	-8.85	
252	188	65,756	-8.85	3	65,949	-7.40	3	66,144	-8.31	191.9
253	189	66,144	-8.31	4	66,429	-6.88	4	66,708	-7.76	192.7
254	189a	66,708	-7.76	2	66,803	-7.54	2	66,898	-7.73	194.5
255	190	66,898	-7.73	3	67,085	-7.22	3	67,272	-7.63	195.3
256	190a	67,272	-7.63	2	67,367	-7.52	2	67,462	-7.80	196.8
257	191	67,462	-7.80	2	67,557	-7.71	3	67,750	-8.15	197.5
258	192	67,750	-8.15	4	68,041	-7.55	3	68,233	-8.27	200.0
259	193	68,233	-8.27	3	68,424	-7.45	2	68,520	-8.01	202.1
260	193a	68,520	-8.01	2	68,617	-7.94	2	68,715	-8.20	203.6
261	194	68,715	-8.20	4	68,987	-5.81	2	69,071	-6.12	205.8
262	195	69,071	-6.12	2	69,155	-5.62	3	69,324	-6.69	206.7
263	195a	69,324	-6.69	2	69,413	-6.92	2	69,506	-7.54	
264	196	69,506	-7.54	4	69,780	-6.55	4	70,054	-7.84	209.9
265	197	70,054	-7.84	3	70,243	-7.05	3	70,425	-7.26	212.0

266	198	70,425	-7.26	3	70,600	-5.67	4	71,013	-5.70	213.8
267	198a	70,848	-5.66	2	70,931	-5.66	5	71,264	-5.99	
268	198b	71,264	-5.99	2	71,347	-5.44	2	71,427	-5.15	
269	199	71,427	-5.15	2	71,506	-4.60	2	71,584	-5.30	219.8
270	200	71,584	-5.30	3	71,743	-4.81	3	71,905	-6.13	220.5
271	201	71,905	-6.13	3	72,079	-5.38	3	72,235	-5.81	222.0
272	201a	72,235	-5.81	2	72,318	-5.82	4	72,578	-6.89	
273	201b	72,578	-6.89	2	72,666	-6.39	2	72,753	-6.64	226.2
274	202	72,753	-6.64	3	72,922	-5.29	4	73,172	-6.31	227.5
275	202a	73,172	-6.31	2	73,258	-6.44	3	73,440	-7.81	
276	203	73,440	-7.81	3	73,620	-6.10	3	73,795	-7.12	227.8
277	204	73,795	-7.12	3	73,973	-6.45	3	74,150	-7.17	228.0
278	204a	74,150	-7.17	3	74,322	-5.91	2	74,405	-5.62	
279	205	74,405	-5.62	2	74,484	-4.74	3	74,651	-6.92	228.4
280	205a	74,651	-6.92	4	74,903	-5.68	2	74,985	-5.61	
281	206	74,985	-5.61	2	75,066	-5.41	2	75,147	-5.72	228.8
282	207	75,147	-5.72	3	75,308	-5.12	3	75,468	-5.41	229.0
283	207a	75,468	-5.41	3	75,625	-4.66	2	75,701	-4.53	
284	208	75,701	-4.53	3	75,850	-4.35	2	75,928	-5.41	227.5
285	209	75,928	-5.41	3	76,084	-4.83	2	76,162	-5.23	227.0
286	210	76,162	-5.23	3	76,313	-4.05	5	76,622	-5.22	226.0
287	211	76,622	-5.22	3	76,777	-4.67	3	76,933	-5.50	224.0
288	212	76,933	-5.50	3	77,094	-5.42	5	77,433	-7.14	223.0
289	213	77,433	-7.14	4	77,687	-5.76	4	77,938	-6.52	221.0
290	213a	77,938	-6.52	2	78,025	-6.62	2	78,113	-7.28	
291	214	78,113	-7.28	3	78,277	-3.82	3	78,437	-6.79	219.2
292	214a	78,437	-6.79	2	78,522	-6.12	2	78,606	-6.32	218.5
293	215	78,606	-6.32	3	78,772	-5.78	3	78,937	-6.24	218.0
294	216	78,937	-6.24	3	79,098	-4.80	3	79,251	-5.00	217.3
295	217	79,251	-5.00	3	79,402	-4.33	3	79,557	-5.50	218.0
296	218	79,557	-5.50	3	79,714	-4.93	3	79,870	-5.41	220.1
297	219	79,870	-5.41	3	80,020	-3.66	3	80,173	-6.38	221.5
298	219a	80,173	-6.38	2	80,257	-6.11	2	80,341	-6.39	222.0
299	220	80,341	-6.39	4	80,572	-4.25	3	80,757	-4.75	223.0
300	221	80,757	-4.75	2	80,869	-4.50	4	81,096	-5.20	224.0
301	222	81,096	-5.20	3	81,240	-3.29	3	81,381	-4.45	225.0
302	223	81,381	-4.45	3	81,523	-3.33	4	81,732	-3.81	226.2
303	223a	81,732	-3.81	3	81,872	-3.73	2	81,942	-3.83	227.5

304	223b	81,942	-3.83	2	82,012	-3.48	2	82,080	-3.56	227.8
305	224	82,080	-3.56	3	82,213	-2.54	3	82,352	-4.85	228.0
306	225	82,352	-4.85	3	82,500	-4.31	3	82,647	-4.75	227.9
307	226	82,647	-4.75	5	82,925	-2.42	2	82,990	-2.98	230.0
308	227	82,990	-2.98	2	83,055	-2.58	5	83,331	-3.94	230.2
309	227a	83,331	-3.94	2	83,401	-3.70	2	83,470	-3.62	
310	228	83,470	-3.62	2	83,538	-3.27	2	83,608	-4.39	233.0
311	229	83,608	-4.39	4	83,814	-3.20	4	84,025	-4.64	235.0
312	230	84,025	-4.64	3	84,203	-3.91	3	84,378	-4.01	237.0
313	231	84,378	-4.01	4	84,576	-1.64	5	84,838	-3.49	239.0
314	232	84,838	-3.49	5	85,100	-2.48	4	85,296	-3.23	239.5
315	233	85,296	-3.23	5	85,551	-2.34	4	85,746	-3.53	238.0
316	233a	85,746	-3.53	2	85,814	-3.42	2	85,881	-3.53	236.0
317	234	85,881	-3.53	4	86,083	-3.38	4	86,286	-3.76	233.0
318	235	86,286	-3.76	2	86,335	-3.64	5	86,635	-4.87	228.1
319	235a	86,635	-4.87	2	86,707	-3.99	2	86,777	-4.35	222.5
320	236	86,777	-4.35	3	86,919	-4.12	4	87,132	-4.49	219.1
321	237	87,132	-4.49	4	87,342	-3.46	3	87,482	-4.83	215.0
322	238	87,482	-4.83	3	87,624	-3.80	2	87,695	-4.55	216.0
323	239	87,695	-4.55	3	87,837	-4.13	3	88,014	-4.43	217.0
324	239a	88,014	-4.43	2	88,049	-4.43	3	88,196	-5.13	
325	239b	88,196	-5.13	7	88,644	-5.03	2	88,719	-5.07	208.0
326	240	88,719	-5.07	4	89,008	-4.10	6	89,373	-5.76	210.0
327	241	89,373	-5.76	3	89,523	-4.69	4	89,748	-5.42	208.2
328	242	89,748	-5.42	4	89,973	-4.69	3	90,128	-6.68	212.0
329	243	90,128	-6.68	3	90,286	-5.34	4	90,517	-5.77	214.0
330	244	90,517	-5.77	4	90,740	-4.16	9	91,336	-5.81	217.0
331	245	91,336	-5.81	3	91,480	-3.53	4	91,685	-4.12	222.0
332	246	91,685	-4.12	2	91,753	-3.85	3	91,896	-4.85	224.5
333	247	91,896	-4.85	2	91,968	-4.59	3	92,114	-5.10	226.0
334	247a	92,114	-5.10	2	92,187	-4.71	2	92,259	-4.54	
335	248	92,259	-4.54	2	92,329	-3.99	3	92,470	-4.94	228.0
336	248a	92,470	-4.94	2	92,542	-4.77	2	92,617	-5.45	228.5
337	249	92,617	-5.45	3	92,759	-3.32	3	92,897	-4.46	228.6
338	250	92,897	-4.46	2	92,967	-4.06	4	93,180	-5.15	228.8
339	251	93,180	-5.15	3	93,325	-4.48	2	93,397	-4.69	299.2
340	252	93,397	-4.69	2	93,468	-4.44	3	93,615	-5.61	229.4
341	253	93,615	-5.61	5	93,895	-3.27	2	93,961	-3.45	229.9

342	254	93,961	-3.45	2	94,026	-3.25	3	94,163	-4.97	230.0
343	255	94,163	-4.97	6	94,517	-3.51	4	94,725	-4.45	231.0
344	256	94,725	-4.45	4	94,932	-3.80	5	95,214	-4.90	231.5
345	257	95,214	-4.90	3	95,351	-3.39	4	95,556	-4.00	232.1
346	258	95,556	-4.00	5	95,828	-3.70	4	96,033	-4.30	231.0
347	259	96,033	-4.30	3	96,204	-3.50	7	96,652	-4.35	230.2
348	260	96,652	-4.35	2	96,722	-3.88	4	96,933	-4.51	229.8
349	261	96,933	-4.51	3	97,075	-4.42	2	97,148	-5.24	229.5
350	262	97,148	-5.24	3	97,294	-4.35	3	97,439	-5.46	229.1
351	263	97,439	-5.46	5	97,727	-3.36	5	98,010	-5.38	228.4
352	264	98,010	-5.38	3	98,157	-4.38	3	98,300	-4.84	228.0
353	265	98,300	-4.84	4	98,505	-3.51	4	98,712	-4.75	227.6
354	265a	98,712	-4.75	2	98,783	-4.39	2	98,855	-4.56	227.4
355	266	98,855	-4.56	3	98,944	-3.80	3	99,134	-4.58	227.2
356	267	99,134	-4.58	8	99,622	-3.92	2	99,691	-4.08	226.2
357	268	99,691	-4.08	6	100,028	-3.45	4	100,232	-4.08	227.4
358	269	100,232	-4.08	3	100,400	-3.11	3	100,565	-3.68	229.0
359	270	100,565	-3.68	5	100,835	-3.42	2	100,902	-3.64	230.9
360	270a	100,902	-3.64	5	101,168	-3.18	2	101,234	-3.18	
361	271	101,234	-3.18	5	101,490	-2.58	2	101,554	-2.96	235.5
362	272	101,554	-2.96	3	101,681	-2.27	3	101,806	-2.49	236.5
363	273	101,806	-2.49	5	102,052	-1.97	3	102,177	-2.86	236.0
364	274	102,177	-2.86	5	102,427	-2.11	5	102,684	-3.32	233.0
365	275	102,684	-3.32	3	102,812	-2.33	3	102,942	-3.55	231.0
366	276	102,942	-3.55	3	103,073	-2.61	3	103,205	-3.78	230.0
367	277	103,205	-3.78	3	103,341	-3.55	3	103,481	-4.52	228.2
368	277a	103,481	-4.52	4	103,697	-4.41	2	103,769	-4.50	230.5
369	278	103,769	-4.50	7	104,195	-4.05	3	104,337	-4.40	230.9
370	278a	104,337	-4.40	2	104,480	-4.32	3	104,623	-4.33	233.5
371	279	104,623	-4.33	4	104,837	-4.17	3	104,982	-4.85	236.0
372	280	104,982	-4.85	5	105,271	-4.10	5	105,559	-4.71	236.6
373	280a	105,559	-4.71	3	105,702	-3.93	2	105,772	-3.93	
374	281	105,772	-3.93	6	106,114	-2.71	5	106,391	-4.48	231.4
375	282	106,391	-4.48	3	106,535	-4.04	5	106,828	-5.07	232.0
376	283	106,828	-5.07	4	107,048	-4.40	5	107,431	-6.48	236.0
377	283a	107,431	-6.48	4	107,683	-6.48	6	108,111	-6.95	
378	283b	108,111	-6.95	3	108,283	-6.71	2	108,369	-6.71	
379	284	108,369	-6.71	6	108,872	-6.28	5	109,249	-6.81	244.0

380	285	109,249	-6.81	4	109,543	-6.09	4	109,790	-6.30	248.8
381	286	109,790	-6.30	3	110,388	-5.58	6	110,829	-6.42	251.6
382	287	110,829	-6.42	8	111,399	-5.68	6	111,847	-6.37	257.4
383	288	111,847	-6.37	11	112,708	-5.67	3	112,872	-6.06	265.5
384	289	112,872	-6.06	8	113,425	-4.85	5	113,736	-5.62	261.8
385	290	113,736	-5.62	6	114,115	-4.33	3	114,264	-4.39	274.4
386	291	114,264	-4.39	3	114,411	-4.24	3	114,562	-4.95	273.8
387	292	114,562	-4.95	7	115,006	-3.45	3	115,150	-4.32	272.0
388	293	115,150	-4.32	5	115,453	-2.47	6	115,886	-3.57	268.8
389	294	115,886	-3.57	5	116,161	-2.86	2	116,228	-2.88	262.5
390	294a	116,228	-2.88	5	116,497	-2.67	3	116,630	-2.67	
391	295	116,630	-2.67	7	117,047	-1.44	3	117,202	-1.83	264.9
392	296	117,202	-1.83	3	117,326	-1.36	3	117,451	-2.00	266.3
393	297	117,451	-2.00	3	117,575	-0.98	6	117,886	-1.88	267.9
394	298	117,886	-1.88	6	118,194	-0.93	4	118,376	-1.46	272.0
395	299	118,376	-1.46	6	118,676	-0.31	3	118,796	-1.77	273.3
396	300	118,796	-1.77	6	119,101	-0.51	3	119,221	-1.40	273.0
397	301	119,221	-1.40	5	119,467	-1.07	3	119,589	-1.31	271.0
398	302	119,589	-1.31	3	119,710	-0.68	3	119,863	-1.47	268.0
399	303	119,831	-1.47	3	120,016	-0.86	3	120,138	-1.29	265.2
400	303a	120,138	-1.29	3	120,259	-0.87	3	120,379	-0.86	
401	304	120,379	-0.86	5	120,612	0.13	5	120,900	-0.59	276.2
402	304a	120,900	-0.59	2	120,959	-0.58	3	121,079	-0.93	276.3
403	305	121,079	-0.93	3	121,256	0.00	3	121,373	-0.65	275.1
404	305a	121,373	-0.65	6	121,727	-0.03	2	121,784	-0.30	
405	306	121,784	-0.30	4	121,951	0.59	3	122,064	-0.37	272.2
406	307	122,064	-0.37	5	122,290	0.50	4	122,430	0.13	274.8
407	308	122,430	0.13	3	122,571	0.39	5	122,891	-0.75	276.3
408	309	122,891	-0.75	3	122,919	-0.09	4	123,095	-0.51	275.0
409	310	123,095	-0.51	5	123,322	1.02	3	123,432	0.22	273.0
410	310a	123,432	0.22	3	123,545	0.34	3	123,658	0.16	271.5
411	311	123,658	0.16	4	123,825	0.72	4	123,991	0.40	269.0
412	312	123,991	0.40	3	124,100	1.24	2	124,154	0.59	266.45
413	312a	124,154	0.59	3	124,265	0.60	3	124,376	0.40	266.4
414	312b	124,376	0.40	5	124,599	0.65	4	124,765	0.60	279.4
415	313	124,765	0.60	2	124,821	0.65	3	124,935	-0.14	278.5
416	314	124,935	-0.14	7	125,271	1.22	3	125,380	0.61	275.5
417	315	125,380	0.61	5	125,598	1.11	3	125,708	0.43	275.0

418	316	125,708	0.43	4	125,877	0.61	5	126,160	0.17	272.9
419	317	126,160	0.17	3	126,272	1.03	5	126,491	0.90	265.0
420	318	126,491	0.90	6	126,749	2.74	3	126,851	1.41	262.6
421	319	126,851	1.41	3	126,955	2.07	4	127,108	2.04	266.0
422	320	127,108	2.04	7	127,410	2.46	3	127,510	2.29	274.5
423	321	127,510	2.29	3	127,610	2.52	3	127,710	2.22	275.0
424	322	127,710	2.22	3	127,810	2.58	4	127,961	2.06	274.7
425	323	127,961	2.06	4	128,112	2.72	4	128,259	2.50	274.3
426	324	128,259	2.50	3	128,357	3.23	3	128,453	3.08	280.0
427	324a	128,453	3.08	2	128,501	3.06	5	128,702	1.87	
428	325	128,702	1.87	3	128,804	2.45	7	129,119	1.39	285.5
429	326	129,119	1.39	5	129,324	2.78	4	129,486	-0.31	270.0
430	327	129,486	-0.31	5	129,705	2.16	6	129,971	1.14	263.7
431	328	129,971	1.14	3	130,079	1.81	4	130,241	0.68	262.0
432	329	130,241	0.68	2	130,297	0.88	3	130,410	0.59	260.0
433	329a	130,410	0.59	3	130,525	0.53	3	130,641	0.24	
434	329b	130,641	0.24	2	130,699	0.14	5	130,942	-0.54	
435	329c	130,942	-0.54	3	131,066	-0.58	2	131,128	-0.79	
436	330	131,128	-0.79	3	131,250	0.16	5	131,506	-1.94	247.5
437	331	131,506	-1.94	5	131,773	-1.45	3	131,908	-2.28	240.4
438	332	131,908	-2.28	2	131,978	-2.23	3	132,120	-2.78	237.8
439	333	132,120	-2.78	4	132,335	-2.42	4	132,548	-2.57	234.5
440	333a	132,548	-2.57	3	132,691	-2.58	6	133,065	-3.84	
441	334	133,065	-3.84	3	133,219	-3.54	3	133,374	-3.93	226.5
442	335	133,374	-3.93	4	133,566	-3.23	3	133,759	-4.41	222.0
443	335a	133,759	-4.41	3	133,923	-4.47	3	134,091	-5.28	
444	335b	134,091	-5.28	2	134,178	-5.40	4	134,447	-6.09	
445	336	134,447	-6.09	3	134,628	-5.74	3	134,815	-6.97	207.0
446	337	134,815	-6.97	3	135,009	-6.88	4	135,308	-7.48	204.6
447	338	135,308	-7.48	3	135,507	-6.83	4	135,802	-7.33	200.2
448	339	135,802	-7.33	3	136,003	-7.14	3	136,206	-7.81	201.8
449	340	136,206	-7.81	3	136,411	-7.39	2	136,512	-7.54	200.0
450	341	136,512	-7.54	2	136,614	-7.29	3	136,819	-7.94	195.9
451	342	136,819	-7.94	3	137,026	-7.50	4	137,341	-7.98	195.1
452	343	137,341	-7.98	3	137,549	-7.45	7	138,193	-9.24	193.6
453	344	138,193	-9.24	3	138,420	-8.59	2	138,532	-8.72	191.0
454	345	138,532	-8.72	5	139,033	-8.30	3	139,197	-8.53	192.0
455	346	139,197	-8.53	3	139,363	-8.40	3	139,643	-8.86	192.2

456	347	139,643	-8.86	3	139,868	-8.43	3	140,093	-8.99	194.6
457	348	140,093	-8.99	3	140,319	-8.34	3	140,542	-8.67	195.0
458	349	140,542	-8.67	4	140,876	-8.11	3	141,100	-8.75	196.0
459	350	141,100	-8.75	3	141,323	-8.31	3	141,547	-8.70	196.5
460	351	141,547	-8.70	4	141,885	-8.39	2	141,997	-8.54	193.2
461	352	141,997	-8.54	3	142,218	-8.12	2	142,329	-8.36	190.65
462	353	142,329	-8.36	2	142,440	-8.25	3	142,665	-8.73	190.5
463	354	142,665	-8.73	5	143,117	-8.09	4	143,450	-8.34	192.0
464	354a	143,450	-8.34	2	143,562	-8.34	3	143,790	-8.87	
465	355	143,790	-8.87	3	144,016	-7.95	2	144,126	-8.18	193.0
466	356	144,126	-8.18	3	144,346	-7.71	6	144,894	-8.32	194.8
467	357	144,894	-8.32	3	145,116	-7.90	5	145,563	-8.62	196.9
468	358	145,563	-8.62	3	145,792	-8.34	2	145,905	-8.45	196.75
469	358a	145,905	-8.45	3	146,131	-8.00	2	146,242	-7.99	
470	359	146,242	-7.99	3	146,461	-7.71	4	146,792	-8.02	196.5
471	359a	146,792	-8.02	3	147,014	-7.88	3	147,236	-8.02	196.0
472	359b	147,236	-8.02	2	147,347	-8.02	2	147,459	-8.15	
473	360	147,459	-8.15	2	147,684	-7.97	5	148,141	-8.45	195.0
474	361	148,141	-8.45	3	148,362	-7.52	2	148,471	-7.70	194.3
475	361a	148,471	-7.70	2	148,581	-7.64	3	148,802	-7.84	194.0
476	361b	148,802	-7.84	4	149,132	-7.54	2	149,241	-7.67	193.8
477	362	149,241	-7.67	3	149,460	-7.46	2	149,569	-7.66	193.5
478	363	149,569	-7.66	6	150,116	-7.33	2	150,224	-7.54	192.2
479	364	150,224	-7.54	3	150,440	-6.93	3	150,653	-7.43	191.9
480	365	150,653	-7.43	3	150,972	-6.61	3	151,181	-6.91	191.5
481	365b	151,181	-6.91	2	151,287	-6.91	3	151,502	-7.42	
482	366	151,502	-7.42	3	151,611	-7.38	5	152,058	-7.89	191.1
483	367	152,058	-7.89	2	152,171	-7.69	3	152,398	-8.15	190.8
484	368	152,398	-8.15	5	152,852	-7.49	2	152,963	-7.67	190.6
485	368a	152,963	-7.67	2	153,076	-7.64	2	153,188	-7.78	190.5
486	369	153,188	-7.78	3	153,412	-7.23	4	153,753	-8.10	190.4
487	370	153,753	-8.10	3	153,981	-7.62	2	154,094	-7.72	190.0
488	370a	154,094	-7.72	2	154,207	-7.64	2	154,322	-8.14	189.9
489	371	154,322	-8.14	3	154,551	-7.37	3	154,783	-9.00	188.8
490	372	154,783	-9.00	3	155,029	-8.53	2	155,151	-8.84	188.0
491	373	155,151	-8.84	2	155,271	-8.06	4	155,625	-8.40	185.5
492	374	155,625	-8.40	2	155,743	-7.89	3	155,983	-8.87	188.0
493	375	155,983	-8.87	2	156,105	-8.28	3	156,349	-9.08	188.5

494	376	156,349	-9.08	3	156,593	-8.17	2	156,714	-8.52	190.0
495	376a	156,714	-8.52	2	156,835	-8.49	2	157,080	-8.58	190.8
496	376b	157,080	-8.58	2	157,202	-8.50	2	157,324	-8.59	191.2
497	377	157,324	-8.59	3	157,560	-7.69	2	157,677	-7.91	193.0
498	378	157,677	-7.91	2	157,793	-7.67	3	158,026	-7.93	194.5
499	379	158,026	-7.93	4	158,359	-6.63	3	158,584	-8.05	197.0
500	380	158,584	-8.05	4	158,925	-6.62	2	159,033	-6.72	198.5
501	381	159,033	-6.72	3	159,240	-5.27	3	159,444	-6.58	199.5
502	382	159,444	-6.58	2	159,548	-5.36	4	159,865	-6.54	200.2
503	383	159,865	-6.54	2	159,971	-5.94	3	160,184	-6.76	201.8
504	384	160,184	-6.76	2	160,293	-6.67	4	160,626	-7.40	202.2
505	384a	160,626	-7.40	2	160,740	-6.85	2	160,851	-7.07	202.2
506	385	160,851	-7.07	2	160,963	-6.79	2	161,077	-7.48	201.5
507	386	161,077	-7.48	2	161,192	-7.34	3	161,427	-7.97	200.4
508	386a	161,427	-7.97	2	161,545	-7.41	2	161,661	-7.38	
509	387	161,661	-7.38	2	161,776	-7.03	2	161,890	-7.25	198.5
510	387a	161,890	-7.25	3	162,172	-6.60	2	162,227	-6.60	
511	388	162,227	-6.60	3	162,440	-5.46	3	162,647	-6.60	194.0
512	389	162,647	-6.60	3	162,867	-6.14	3	163,089	-7.25	191.7
513	389a	163,089	-7.25	2	163,204	-7.03	2	163,318	-7.05	191.0
514	390	163,318	-7.05	3	163,546	-6.81	2	163,660	-7.23	190.0
515	390a	163,660	-7.23	2	163,777	-7.39	2	163,896	-7.66	
516	391	163,896	-7.66	3	164,136	-7.58	4	164,642	-8.77	188.0
517	392	164,642	-8.77	2	164,769	-8.11	3	165,021	-8.44	186.0
518	392a	165,021	-8.44	2	165,148	-8.30	2	165,274	-8.31	184.5
519	393	165,274	-8.31	2	165,399	-7.82	4	165,774	-8.57	183.8
520	394	165,774	-8.57	3	166,029	-7.97	2	166,155	-8.44	187.5
521	395	166,155	-8.44	3	166,411	-8.12	2	166,537	-8.34	188.0
522	396	166,537	-8.34	2	166,662	-7.65	2	166,785	-7.90	188.8
523	396a	166,785	-7.90	2	166,909	-7.82	2	167,035	-8.45	189.0
524	397	167,035	-8.45	4	167,414	-7.76	2	167,539	-7.96	191.0
525	397a	167,539	-7.96	2	167,664	-7.96	2	167,790	-8.05	
526	398	167,790	-8.05	6	168,391	-6.62	2	168,506	-6.90	194.0
527	399	168,506	-6.90	2	168,623	-6.71	3	168,857	-7.05	195.0
528	399a	168,857	-7.05	3	169,088	-6.33	2	169,145	-6.33	
529	400	169,145	-6.33	4	169,531	-5.08	4	169,866	-6.87	197.5
530	401	169,866	-6.87	2	169,983	-6.61	3	170,221	-7.30	197.9
531	402	170,221	-7.30	4	170,568	-6.05	3	170,803	-7.25	197.9

532	403	170,803	-7.25	2	170,922	-6.61	3	171,165	-7.97	197.8
533	404	171,165	-7.97	3	171,405	-6.16	3	171,638	-7.41	197.8
534	405	171,638	-7.41	2	171,760	-6.88	5	172,262	-8.15	197.8
535	406	172,262	-8.15	3	172,522	-7.53	3	172,774	-7.64	197.8
536	406a	172,774	-7.64	2	172,900	-7.51	2	173,027	-7.72	197.5
537	407	173,027	-7.72	3	173,275	-6.89	2	173,397	-7.11	196.8
538	407a	173,397	-7.11	2	173,519	-6.96	2	173,642	-7.13	196.0
539	408	173,642	-7.13	3	173,875	-5.74	3	174,105	-6.86	195.0
540	409	174,105	-6.86	4	174,573	-5.95	3	174,804	-6.27	193.8
541	410	174,804	-6.27	2	174,920	-5.92	3	175,150	-6.14	191.5
542	410a	175,150	-6.14	2	175,266	-6.16	3	175,509	-7.25	
543	411	175,509	-7.25	3	175,746	-6.04	3	175,991	-7.22	190.4
544	411a	175,991	-7.22	2	176,117	-7.23	2	176,244	-7.56	
545	412	176,244	-7.56	2	176,373	-7.33	3	176,630	-7.58	191.0
546	413	176,630	-7.58	3	176,887	-7.19	2	177,015	-7.49	196.0
547	414	177,015	-7.49	4	177,393	-6.88	4	177,773	-7.44	199.0
548	415	177,773	-7.44	2	177,900	-6.94	5	178,417	-8.19	203.5
549	415a	178,417	-8.19	2	178,554	-8.15	3	178,830	-8.35	207.7
550	416	178,830	-8.35	4	179,217	-6.65	2	179,342	-7.00	209.8
551	417	179,342	-7.00	4	179,706	-5.30	3	179,939	-6.39	210.2
552	417a	179,939	-6.39	4	180,304	-6.28	2	180,426	-6.44	212.0
553	418	180,426	-6.44	5	180,895	-5.32	4	181,259	-6.92	213.9
554	419	181,259	-6.92	2	181,382	-5.80	3	181,626	-6.77	216.0
555	420	181,626	-6.77	2	181,753	-6.71	5	182,284	-8.00	216.0
556	421	182,284	-8.00	2	182,421	-7.52	2	182,694	-8.08	210.0
557	422	182,694	-8.08	2	182,830	-7.29	2	182,965	-7.70	206.2
558	422a	182,965	-7.70	2	183,102	-7.77	2	183,243	-8.58	
559	423	183,243	-8.58	3	183,525	-7.64	3	183,807	-8.20	200.1
560	424	183,807	-8.20	3	184,088	-7.79	2	184,229	-8.10	201.0
561	425	184,229	-8.10	3	184,501	-7.10	2	184,641	-8.72	202.0
562	426	184,641	-8.72	3	184,928	-7.75	3	185,212	-8.23	203.5
563	427	185,212	-8.23	2	185,354	-7.75	3	185,640	-8.72	204.0
564	428	185,640	-8.72	3	185,931	-7.64	3	186,213	-7.98	206.2
565	428a	186,213	-7.98	2	186,356	-7.95	2	186,499	-8.14	208.0
566	429	186,499	-8.14	2	186,642	-7.68	2	186,784	-8.09	209.0
567	430	186,784	-8.09	4	187,204	-7.27	3	187,486	-8.14	210.7
568	431	187,486	-8.14	4	187,907	-7.01	3	188,181	-7.87	217.5
569	432	188,181	-7.87	3	188,467	-7.63	2	188,609	-7.92	222.0

570	432a	188,609	-7.92	2	188,752	-7.51	2	188,892	-7.46	
571	433	188,892	-7.46	4	189,297	-6.48	2	189,431	-7.08	231.4
572	434	189,431	-7.08	4	189,832	-6.02	3	190,092	-6.49	231.4
573	434a	190,092	-6.49	4	190,469	-4.84	2	190,587	-4.79	
574	435	190,587	-4.79	4	190,934	-3.60	7	191,647	-5.55	231.5
575	435a	191,647	-5.55	2	191,771	-5.36	2	191,895	-5.46	226.0
576	436	191,895	-5.46	3	192,138	-4.83	5	192,638	-6.01	222.0
577	437	192,638	-6.01	3	192,895	-5.35	3	193,152	-6.21	218.2
578	437a	193,152	-6.21	2	193,285	-6.28	2	193,421	-6.78	
579	438	193,421	-6.78	3	193,687	-5.68	2	193,816	-5.89	219.0
580	439	193,816	-5.89	6	194,444	-4.53	2	194,565	-4.96	219.4
581	440	194,565	-4.96	3	194,806	-4.23	3	195,051	-5.22	219.5
582	441	195,051	-5.22	3	195,298	-4.81	5	195,808	-5.95	220.0
583	441a	195,808	-5.95	2	195,940	2.00	2	196,071	-5.73	
584	442	196,071	-5.73	2	196,202	-5.59	3	196,463	-5.72	223.0
585	442a	196,463	-5.72	2	196,593	-5.45	2	196,722	-5.37	
586	443	196,722	-5.37	3	196,965	-4.04	3	197,211	-5.17	228.2
587	444	197,211	-5.17	3	197,462	-4.79	2	197,587	-4.87	232.0
588	445	197,587	-4.87	3	197,833	-4.30	2	197,954	-4.48	234.0
589	446	197,954	-4.48	4	198,309	-3.80	2	198,426	-3.81	238.0
590	447	198,426	-3.81	3	198,656	-3.20	2	198,768	-3.29	240.0
591	448	198,768	-3.29	3	198,992	-2.96	3	199,220	-3.84	242.6
592	449	199,220	-3.84	3	199,452	-3.40	2	199,567	-3.63	244.0
593	450	199,567	-3.63	3	199,793	-2.80	2	199,904	-2.95	244.5
594	451	199,904	-2.95	2	200,015	-2.68	3	200,236	-3.07	245.5
595	452	200,236	-3.07	3	200,451	-2.02	2	200,558	-2.42	246.5
596	452a	200,558	-2.42	2	200,666	-2.48	2	200,776	-2.82	
597	453	200,776	-2.82	6	201,319	-1.49	3	201,529	-2.11	249.0
598	453a	201,529	-2.11	2	201,635	-1.99	2	201,742	-2.26	249.5
599	453b	201,742	-2.26	2	201,849	-2.08	2	201,957	-2.34	250.0
600	454	201,957	-2.34	3	202,169	-1.53	3	202,386	-2.59	251.0
601	454a	202,386	-2.59	2	202,496	-2.51	2	202,607	-2.54	247.5
602	455	202,607	-2.54	3	202,826	-2.29	2	202,936	-2.49	244.0
603	456	202,936	-2.49	4	203,262	-1.90	3	203,281	-2.56	240.8
604	457	203,281	-2.56	2	203,592	-2.43	5	204,049	-3.10	242.5
605	458	204,049	-3.10	2	204,164	-2.71	3	204,394	-3.25	248.0
606	459	204,394	-3.25	4	204,743	-2.56	5	205,214	-3.69	246.0
607	460	205,214	-3.69	3	205,458	-3.63	3	205,708	-4.25	237.5

608	460a	205,708	-4.25	3	205,965	-4.45	3	206,232	-5.05	
609	461	206,232	-5.05	3	206,496	-4.39	3	206,759	-4.65	231.0
610	462	206,759	-4.65	2	206,890	-4.27	2	207,019	-4.37	233.0
611	462a	207,019	-4.37	2	207,149	-4.29	3	207,409	-4.49	235.0
612	462b	207,409	-4.49	2	207,540	-4.37	3	207,803	-4.51	237.0
613	463	207,803	-4.51	3	208,061	-4.02	2	208,191	-4.35	239.0
614	464	208,191	-4.35	2	208,319	-3.70	2	208,445	-3.81	240.0
615	464a	208,445	-3.81	3	208,696	-3.59	4	209,072	-3.70	240.4
616	465	209,072	-3.70	3	209,315	-2.88	4	209,686	-3.73	241.6
617	465a	209,686	-3.73	2	209,812	-3.48	2	209,938	-3.58	244.0
618	466	209,938	-3.58	3	210,182	-2.51	2	210,300	-2.64	245.0
619	466a	210,300	-2.64	2	210,418	-2.67	2	210,538	-2.91	
620	467	210,538	-2.91	4	210,893	-2.14	4	211,246	-2.67	247.3
621	467a	211,246	-2.67	2	211,366	-2.56	2	211,485	-2.53	
622	468	211,485	-2.53	2	211,603	-2.28	3	211,842	-2.80	253.5
623	468a	211,842	-2.80	2	211,960	-2.00	2	212,075	-2.03	255.0
624	469	212,075	-2.03	2	212,190	-1.81	2	212,305	-2.17	257.0
625	470	212,305	-2.17	5	212,766	-1.63	2	212,881	-2.07	256.0
626	471	212,881	-2.07	3	213,109	-1.50	2	213,223	-1.96	255.0
627	472	213,223	-1.96	3	213,453	-1.67	3	213,684	-2.06	254.0
628	473	213,684	-2.06	3	213,911	-1.35	2	214,024	-1.58	252.0
629	474	214,024	-1.58	3	214,251	-1.40	3	214,478	-1.61	250.2
630	475	214,478	-1.61	4	214,819	-1.29	3	215,047	-1.67	243.8
631	476	215,047	-1.67	5	215,497	-0.91	3	215,723	-1.74	240.9
632	477	215,723	-1.74	2	215,839	-1.45	4	216,197	-2.39	242.7
633	477a	216,197	-2.39	2	216,319	-2.11	2	216,439	-2.14	247.0
634	478	216,439	-2.14	4	216,904	-0.97	2	217,018	-1.23	250.0
635	479	217,018	-1.23	3	217,244	-0.86	4	217,584	-1.20	251.2
636	480	217,584	-1.20	2	217,699	-1.18	2	217,817	-2.18	245.4
637	481	217,817	-2.18	3	218,060	-1.85	3	218,303	-2.08	242.0
638	481a	218,303	-2.08	2	218,426	-2.20	3	218,681	-3.23	
639	482	218,681	-3.23	4	219,076	-2.90	4	219,472	-3.35	226.0
640	483	219,472	-3.35	2	219,605	-2.84	3	219,878	-4.37	216.0
641	484	219,878	-4.37	3	220,167	-4.23	3	220,461	-4.99	216.2
642	485	220,461	-4.99	3	220,761	-4.35	3	221,058	-5.03	208.0
643	486	221,058	-5.03	2	221,210	-4.89	4	221,684	-6.19	208.0
644	487	221,684	-6.19	2	221,850	-6.02	5	222,535	-7.29	206.0
645	488	222,535	-7.29	2	222,711	-6.49	4	223,062	-7.02	203.5

646	489	223,062	-7.02	2	223,240	-6.89	3	223,605	-7.63	210.0
647	490	223,605	-7.63	4	224,164	-7.36	2	224,351	-7.64	227.5
648	491	224,351	-7.64	4	224,888	-5.89	2	225,058	-6.22	236.5
649	492	225,058	-6.22	4	225,562	-4.99	3	225,900	-6.59	234.0
650	493	225,900	-6.59	3	226,238	-5.58	2	226,408	-6.17	228.0

Source data and measurements on all centennial-scale temperature-proxy oscillations (ACOs, or TO_{C350V} cycles) from Vostok ice-core data, 226,408 to 149 yb1950. CO_2 values in parentheses for the most recent 3,646 years are interpolated from the more highly-resolved and nearby EPICA Dome C climate record (AICC2012 chronology matched to Vostok AICC2012 TO_{C350V} cycle peaks). The CO_2 data were not used in this paper. The contents of the table are explained in column headings. Time reads backward from left to right in each row consistent with the timescales in all figures. The fifth and eighth columns, entitled respectively “# cooling datapoints” and “# warming datapoints,” document compliance of the data utilized in this study with the Nyquist-Shannon sampling-frequency criterion discussed above in SM section 2. **Methods**, 2.3. *Frequency Aliasing*, p. 2. These two columns are partially redundant in that values for the warming and cooling phases both include datapoints at peak of each TO_{C350V} cycle, i.e. the datapoint corresponding to the cycle peak is counted twice. The total number of datapoints (T_D) comprising each TO_{C350V} cycle is therefore one less than the sum of datapoints in the two columns, or:

$$T_D = [(\# \text{ cooling datapoints}) + (\# \text{ warming datapoints})] - 1 \quad (19)$$

Measurements on all centennial-scale temperature oscillations (TO_{C350V} cycles) in the Vostok ice-core record from 226,408 to 149 yb1950 are from the GT4 glaciological chronology [1,2]. All TO_{C350V} cycle properties summarized in this paper were computed from and can be replicated using this database. The CO_2 values enclosed in parentheses (cycles 1-28) are linearly-interpolated values from the EDC3 AICC2012 chronology [3] matched to peak times of Vostok AICC2012 cycles. The color of the font designates the method of defining the corresponding TO_{C350V} cycles as follows: Black, TO_{C350V} cycles larger than 0.25 °C in amplitude (definition 1 in main paper, section 2. Methods); red, TO_{C350V} cycles from 0.045 to 0.25 °C in amplitude (definition 2); blue, TO_{C350V} cycles identified as a positive inflection in the temperature record followed by a negative inflection (definition 3); green, atmospheric carbon dioxide (CO_2), with the time of occurrence interpolated linearly to the time of nearest temperature-proxy datapoint between adjacent CO_2 measurements. CO_2 was determined only for TO_{C350V} cycles identified using the first and second definitions, for which amplitude and rates of temperature change could be computed. Abbreviations: yb, years before; ΔT , temperature anomaly from 1960-1990 (the reference time period used in the original Vostok data).